Active matter therapeutics

Arijit Ghosh, Weinan Xu, 1,# Neha Gupta, David H. Gracias 1,2,*

¹Department of Chemical and Biomolecular Engineering, Johns Hopkins University, Baltimore, Maryland 21218, USA

²Department of Materials Science and Engineering, Johns Hopkins University, Baltimore, Maryland 21218, USA

*Present address: Department of Polymer Engineering, University of Akron, Akron, Ohio 44325, USA

*Corresponding Author email: dgracias@jhu.edu

Keywords: nanotechnology, nanomotors, cancer, drug delivery, clot removal, tumor transport.

ABSTRACT

Nanotherapies based on micelles, liposomes, polymersomes, nanocapsules, magnetic nanoparticles, and noble metal nanoparticles have been at the forefront of drug delivery in the past few decades. Some of these nanopharmaceuticals have been commercially applied to treat a wide range of diseases, from dry eye syndrome to cancer. However, the majority involve particles that are passive, meaning that they do not change shape, and they lack motility; the static features can limit their therapeutic efficacy. In this review, we take a critical look at an emerging field that seeks to utilize active matter for therapeutics. In this context, active matter can be broadly referred to as micro or nanosized constructs that energetically react with their environment or external fields and translate, rotate, vibrate or change shape. Essentially, the recent literature suggests that such particles could significantly augment present-day drug delivery, by enhancing transport and increasing permeability across anatomical barriers by transporting drugs within solid tumor microenvironments or disrupting cardiovascular plaque. We discuss examples of such particles and link the transport and permeability properties of active matter to potential therapeutic applications in the context of two major diseases, namely cancer and heart disease. We also discuss potential challenges, opportunities, and translational hurdles.

1. Introduction

Conventionally, active matter refers to collections of particles that dissipate energy and are out of equilibrium [1,2]. Some examples of active matter in nature include motor protein collections, bacterial colonies, tissues, bird flocks, fish schools, and animal herds [3]. Examples of synthetic active matter include vibrating copper rods [4] and self-propelled nano to millimeter sized particles [5,6]. Active matter has been extensively studied in colloidal science, non-equilibrium thermodynamics, and self-assembly since it is well known that the dissipation of energy can drive self-organization and cause order to spontaneously emerge out of disorder at a variety of length scales [7].

In this review, we use a broad definition of active matter and include particles that are both self-driven and externally propelled. We focus on particles that display translational, rotational, or vibrational motion and shape-change. With recent advances in the synthesis, fabrication, and assembly of complex, multi-functional and tunable micro and nanoparticles, there has been an explosive growth in the study of such dynamic micro and nanosized structures [8–10]. In contrast to passive or static particles, active particles can respond to stimuli, chemicals, or energetic fields in their local environment [11–13] and enhance functionality in application areas ranging from environmental remediation to remote sensing [14–16].

In modern medicine, active matter therapeutics is an emerging field wherein dynamic changes within particles such as propulsion or shape change enhance their therapeutic efficacy [17–19]. In this review, we survey the types of active matter and discuss the potential of these particles in therapeutics, in the context of two important diseases: cancer and heart disease. We discuss the applicability of such particles and structures in low (individual) and high (collections) concentrations. We have organized the review as follows: first, we briefly discuss the historical

trends in therapeutic particles and outline their characteristics. We then outline the transport limitations of conventional nanoparticle therapies to reach the interior of a tumor, which can significantly limit their efficacy. We also discuss the limitations of conventional invasive and non-invasive methods for plaque removal from blood vessels. We then present arguments based on published theoretical models and experiments which suggest that active particles can significantly enhance transport and permeability through tumors and disrupt plaque. These results suggest the possibility to design and apply novel dynamic therapies for the treatment of cancer and heart disease. Finally, we present some clinical translational barriers which mainly include safety concerns and the lack of systematic *in vivo* research data.

2. Progress of nanotherapeutics from a historical perspective

The transport of a drug to its targeted diseased site such as a tumor is critically linked to its therapeutic efficacy. The human body is a labyrinth and has many barriers and mechanisms to clear foreign materials [20]. These barriers isolate fluids and prevent pathogens from invading specific organs. As an example, a significant barrier for orally delivered drugs is the gastrointestinal (GI) epithelial lining which contains tight cell junctions, a specific purpose of which is to isolate GI contents from other parts of the body. In the small intestine, the epithelium folds to form villi, and degradative enzymes within the microvilli further limit the absorption of therapeutic molecules. Consequently the oral delivery of peptide drugs such as insulin *via* the GI tract has proven to be a formidable challenge [21]. Likewise, there are a number of barriers in the central nervous system such as the blood-cerebrospinal fluid (CSF) epithelial barrier, blood-brain endothelial barrier, embryonic CSF-brain barrier, and arachnoid barrier [22,23]. Mucus is also a significant barrier to oral or nasal drug delivery, due to its negative charge and hydrophobic domains, which hinders the free diffusion of therapeutics within and through the mucus. The

mucus layer is also a dynamic barrier because of the continuous secretion and shedding of mucosal surfaces [24]. For instance, the inner mucus layer of the colon has a thickness of several hundred micrometers in humans, and the turnover time is of the order of an hour [25]. The clearance of the drug molecules through the liver, kidney and the spleen also reduces the bioavailability of therapeutics [26]. Drug availability is also limited by immune components such as macrophages that are adept at clearing away foreign objects with a wide range of sizes (submicron to as large as about 5 μ m) [27]. Consequently, targeting a diseased area of the body is a daunting challenge as drug molecules and particles must evade immune components as well as natural clearance mechanisms and selectively pass through barriers.

To place active matter in modern therapeutics from a historical perspective, we classify different generations of drug delivery systems (Fig. 1) [28]. The first generation focused on oral and transdermal delivery using powders and injections that could deliver drugs *via* the GI tract, intravenously, and intramuscularly [29]. Representative examples of drugs developed during this stage include acetylsalicylic acid to treat pain, fever, or inflammation; and doxorubicin to treat cancer (Fig. 1A). By leveraging the significant progress in polymer synthesis, nanotechnology, and self-assembly in the past few decades, scientists developed a second generation of drug delivery systems compose of more complex particles and structures. These included mesoporous particles, micelles, dendrimers, liposomes, polypeptides, hydrogels, and microneedles (Fig. 1B) [30–37]. Second generation drug delivery systems featured new characteristics designed to improve therapeutic efficacy and bioavailability, which included compartmentalization and surface functionalization to prevent premature drug degradation and tunability of dissolution for controlled or programmed release. For example, mesoporous silica particles have very high surface to volume ratios for better drug loading and can be functionalized for optimization and control of

the release characteristics [30, 31]. Efforts were also directed at manipulating shape, size, and particle distribution. For example, several liposomal formulations of doxorubicin were developed with reports of reduced cardiotoxicity and enhanced bioavailability [38,39]. Doxorubicin hydrochloride liposome and liposomal Vitamin C are commercially available and widely utilized.

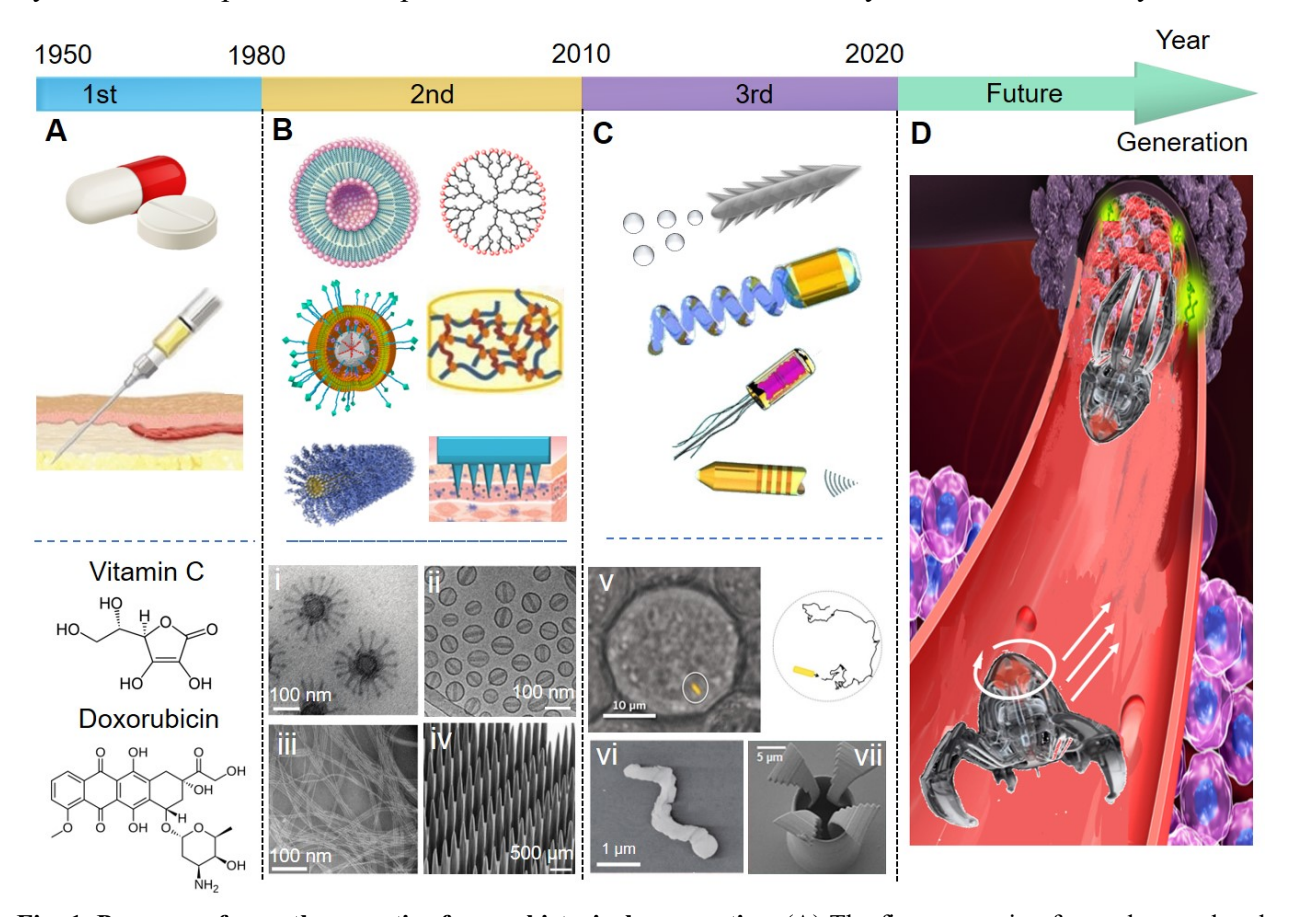


Fig. 1. Progress of nanotherapeutics from a historical perspective. (A) The first generation focused on oral and transdermal delivery, such as with tablets and intravenous injections. (B) The second generation included micro and nanoparticles (including both bottom-up and top-down generated) and hydrogels, such as, (i) micelles, (ii) liposomes, (iii) polypeptides, (iv) and microneedles. Reprinted (adapted) with permission from [49] Copyright (2009) American Chemical Society; [50] Copyright (2012) Elsevier, B.V.;[57] Copyright (2002) National Academy of Sciences; [61] Copyright (2005) Elsevier B.V. (C) The third generation moved beyond passive particles, to include structures with the capability to move and respond inside the body or even a single cell, such as a, (v) nanomotor, (vi), micromotor, and (vii) hybrid micromotor. Reprinted (adapted) with permission from [65,66] Copyright (2014, 2018) WILEY-VCH Verlag GmbH & Co. KGaA, Weinheim; [67] Copyright (2018) American Chemical Society. (D) We anticipate that future drug delivery systems will be based on active matter that combines controlled movement, reconfigurable shape, and integrated functionality.

Elsewhere, by tuning the porosity and consequently the permeability of hydrogels, researchers were able to dramatically alter dosing, stimuli responsivity, and drug release kinetics [33,40,41]. For example, polymers like ethylene vinyl acetate have been loaded with drugs like insulin,

nicotine, or progesterone, and used to temporally control drug release from several days to one year [42,43]. Also, glucose oxidase based sensing has been used in conjunction with amphiphilic polymers to create a glucose sensing capsule that can deliver insulin up to 12 h [44].

The size, shape and surface properties of nanoparticles are readily tunable, which can be utilized to enhance the solubility of drug molecules as well as to leverage the enhanced permeation and retention (EPR) effect for more effective delivery of therapeutics [45–47]. In this regard, it was discovered that the size of nanoparticles has a significant effect on their circulation half-life, macrophage uptake, and extravasation [48]. In general, nanoparticles smaller than 5 nm are rapidly cleared by the kidney after intravenous administration; nanoparticles in the range of 100-200 nm (such as micelles [49] and liposomes [50] shown in **Fig. 1**B) tend to extravasate through vascular fenestrations of tumors, and avoid filtration by the liver and spleen; larger particles, over 2000 nm, easily accumulate in the spleen, liver, and capillaries of the lungs [20]. There are quite a few commercially available nanoparticle-based therapeutics that are United States Food and Drug Administration (FDA) approved. Some examples include pegylated interferon alpha-2a for the treatment of chronic hepatitis C [51] or inorganic nanoparticles such as iron dextran for the treatment of iron deficiency and anemia [52].

The shape of nanoparticles is another critical parameter that affects their cellular uptake, macrophage internalization, and hemorheological behaviors [53]. For instance, it has been observed that nanoparticles with a smaller length-normalized curvature (<45°) undergo faster internalization than nanoparticles with a larger length-normalized curvature [54]. Thus, spherical microparticles or smaller disc shaped particles were found to be more easily internalized (8 - 10 times faster) than ellipsoids or elongated discs or nanorods [55], and the internalization efficiency of differently shaped nanoparticles has been related to the strain energy required for the

deformation of the cell membrane around the nanoparticle [56]. Also, polymer micelles with filamentous geometry have much longer circulating lifetime as compared to spherical micelles [57] due to their ability to be better aligned with blood flow [58].

In addition to nanoparticles formed by bottom-up synthesis or assembly, top-down fabricated nano/microstructures also offer unique advantages in drug delivery. Advanced molding and roll-to-roll based microfabrication techniques such as Particle Replication in Non-wetting Templates (PRINT) allow the design of precisely shaped micro and nanoparticles with independent control over their physical parameters [59,60]. Top-down microfabricated needle arrays have been used for transdermal delivery (**Fig. 1B**) [61] of a range of therapeutics including proteins and vaccines [62]. Several companies have introduced commercial microneedle products, including 3M, that has developed microneedle arrays (Microchannel Skin System) to increase skin permeability before dermatological procedures. Despite the enormous progress, much more needs to be done in order to allow drugs to cross biological barriers to access diseased sites, reduce toxicity, and enhance quality control and reproducibility [63,64].

In order to further enhance the efficiency of drug delivery systems, researchers are looking towards dynamic particles that are either self-propelled or driven by external fields (**Fig. 1**C). In this regard, researchers are inspired by motile cells such as bacteria, which are capable of moving with ease in complex biological environments in the human body. A major thrust is in the development of micro and nanomotors, that can potentially move within the human body either in an autonomous manner or directed by external fields [65,66]. There is already significant progress in the use of such nanomotors for therapeutic payload delivery, isolation of biological targets, and operation within living cells under *in vitro* and *ex vivo* conditions [67]. A few recent reports show preliminary evidence for *in vivo* applicability [18,68,69]. We envision that the future of drug

delivery systems will include not just motile particles, but also those that change shape such as gripping modules shown in **Fig. 1**D [70,71]. We note that shape morphing is an important characteristic to be mimicked in drug delivery, since biological cells themselves can morph as the fluid cell membrane enables facile shape change. Next, we discuss the significant advantages of active matter therapeutics in the context of two drug delivery applications: the delivery of anticancer drugs to the interior of solid tumors and the removal of plaque from blood vessels.

3. Drug delivery to the interior of a solid tumor is a major challenge

The prevailing idea in cancer nanomedicine is that tumors can be selectively targeted because of the enhanced permeability and retention (EPR) effect [72,73]. Due to the high cell growth rate in tumors and release of angiogenesis factors, tumor vasculature is irregular, leaky, tortuous and malformed with hyper permeability [74–76]. Indeed, it has been shown that due to the leaky vasculature present in tumors, macromolecules larger than 40 kDa in size have a higher chance of accumulating and being retained in the tumor stroma as compared to blood vessels in normal tissues (**Fig. 2**A). The discovery of the EPR effect led to a wide range of designs of nanoparticle therapies.

However, a review of the literature over the past few years [77] shows that less than 1% of the injected dose (ID) of particles actually reach the tumors and less than 0.007% of the ID interact with the cancer cells. The situation is similar for passive and targeted nanoparticles alike with marginal improvements in these numbers. While most (> 97%) of the injected nanoparticles are removed by the immune cells to the liver and spleen, the particles that manage to extravasate into the tumor, still cannot reach the tumor interior (**Fig. 2**B - D) especially at increasing distances from the blood vessels because of limitations posed by the interstitial fluid pressure, surface charges, and interactions with macrophages inside the tumor.

Indeed, the solid tumor microenvironment is an extremely complex, multi-cellular environment in a state of dynamic equilibrium [63]. Solid tumors also have poorly functioning lymphatics especially in the interior of the tumor [78]. The tumor pathophysiology shows that the interior of the tumor is associated with low oxygen concentrations (hypoxia) and higher interstitial fluid pressure (IFP, **Fig. 2**B) [79]. Hypoxia has been linked to lower chances of survival in

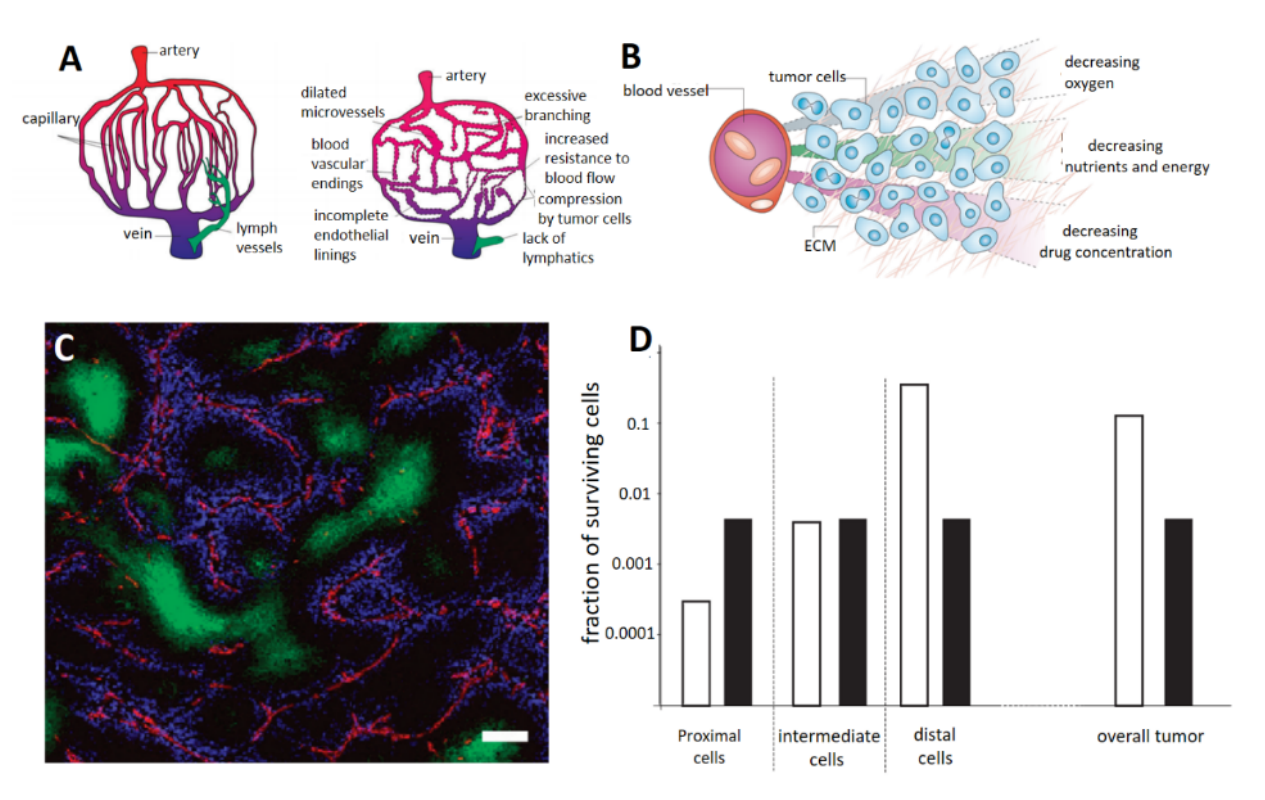


Fig. 2. The solid tumor microenvironment prevents drug transport to the interior. (A) Diagrammatic representation of the vascular system in normal tissue and a solid tumor showing poor arrangement of the blood vessels in the tumor and the lack of lymphatics. Reproduced from [90] by permission of Oxford University Press. Copyright (2007) The Author. (B) Schematic showing the distribution of oxygen, nutrients, and drugs in the tumor interstitium away from a blood vessel. Reproduced with permission from [74]. Copyright (2006) Nature Publishing Group. (C) Perivascular distribution of doxorubicin (blue), in relation to the blood vessels (red) and the hypoxic regions (green)in a tumor tissue section, showing that the anticancer drug fails to penetrate into the hypoxic regions of the tumor. Reproduced with permission from [91]. Copyright (2005) American Association for Cancer Research. (D) Surviving fractions for three tumor cell populations characterized by their proximity to a blood vessel and for the overall tumor cell population, estimated for experimentally determined distribution of doxorubicin (open bars) or by assuming a homogeneous distribution (solid bars). The incorrect assumption of uniform drug distribution leads to a marked overestimation of drug effects to kill cancer cells. Reproduced from [90] by permission of Oxford University Press. Copyright (2007) The Author.

metastatic patients over several months as well as poorer response to radiation and surgery with higher chances of recurrence [80]. It has been hypothesized that in order to improve therapeutic response, drugs need to be delivered to the hypoxic regions of the tumor. As we see below, the state-of-the-art systems of nanotherapeutics that are in clinical or preclinical trials cannot achieve this efficiently due to their inability to overcome several barriers that hinder the transport of these particles. The reader is directed to another review for a detailed analysis and description of these barriers [75]. Briefly, they include:

- a) Clearance by the immune system: While delivering drug to the tumor, the first barrier that any nanoparticle-based approach in the vascular system faces is clearance by the immune system including the liver and spleen. In general, it has been shown that particles smaller than 5 6 nm are more likely to get eliminated from the body within 3 h. It has also been shown that particles of asymmetric shapes or elongated particles are less likely to undergo endocytosis by macrophages. Thus, shape and size of the particle are important considerations for tumor penetration [81–86].
- b) *Hindered diffusion in the extracellular matrix (ECM):* The tumor ECM is a dense network of collagen [87–89] along with other components like glycoproteins. While smaller molecules that are of the size range < 5 nm have a higher chance to diffuse through the matrix, functional drug delivery particles are often larger in size, upto several hundreds of nm, and are significantly slower in their diffusion process through the densely packed ECM [92–95]. The diffusion of large molecules through the tumor interstitium has been linked to the density and distribution of the collagen networks [96]. For example, in a physiologically relevant concentration of 4.5% type I collagen gel, the diffusivity of a 10 nm radius particle has been found [89] to be almost one order of magnitude smaller than that in water.
- c) *Electrostatic interactions:* The collagen network in the ECM carries a slight positive charge which hinders the diffusion of particles that carry negative charges. Conversely, the presence of glycosaminoglycan fibers that carry negative charge is detrimental to positively charged particles.

Studies have shown that the components of the ECM like heparan sulfate can cause charged nanotherapeutic particles to bind to the ECM fibers and reduce the diffusivity by almost three orders of magnitude [97–100].

d) *Interstitial fluid pressure (IFP):* The IFP inside a tumor, as mentioned above, builds up due to the absence of proper drainage of the fluid inside the tumor, due to compromised lymphatics and higher perfusion through the disordered vasculature in the tumor. The increase in the fluid pressure can also be attributed to the difference in composition of the tumor stroma that contains cells of the immune system releasing cytokines [101]. For example, cytokines like the vascular endothelial cell growth factor (VEGF) increase the vascular permeability and thus causes an increased outflow of molecules into the tumor stroma [102]. An increased IFP is observed towards the center of the tumor and the IFP goes down at the boundary [103–105]. This leads to an outward convective interstitial fluid flow and any transport into the tumor is hindered. The transport of the particles is thus only driven by diffusion, which is a slow process considering the high effective viscosity of the ECM [89,103,106,107]. Thus, for efficient drug delivery to the interior of the tumor, it is necessary to overcome the IFP, and alternate sources of convective transport are necessary.

Due to the multivariate problems that can arise in trying to overcome anatomical barriers, many have proposed that nanoparticles must be designed for specific tumor or cancer types to attain an effective therapy [108]. This is because vasculatures around tumors can have different nominal pore sizes, tumors can have different ECM compositions with varying effective viscosity and different tumor cell types can have different surface chemistries. However, cancer nanotherapeutics can benefit greatly if the particles that reach the tumor site can have increased diffusion or can overcome the electrostatic or fluidic forces that they encounter. As noted later, active particles have the potential to drastically improve transport inside the tumor. They can

harness the energy from their surroundings or external sources and convert them into mechanical energy resulting in faster, sustained, and convective motion.

4. Current techniques to remove plaque from blood vessels

Another clinical application that could be addressed using active matter therapeutics is the removal of plaque from blood vessels. Plaque in blood vessels is mainly composed of fat, cholesterol, and other hydrophobic molecules. Plaque can start accumulating in blood vessels as early as childhood and can progressively harden to narrow the lumen in blood vessels and limit blood flow. Oral medication is a common method of combating accumulation of plaque in blood

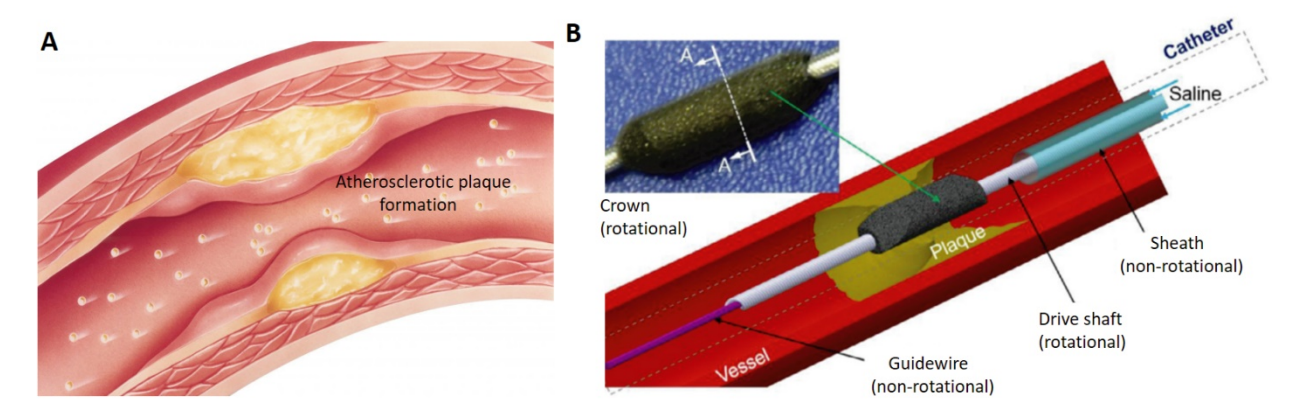


Fig. 3. Conventional non-invasive and surgical methods to remove plaque from blood vessels. (A) Schematic representation of statin therapy for atherosclerotic cardio-vascular disease. Image credit: Intermountain Healthcare Heart Institute. (B) Schematic showing the use of a surgical technique, orbital atherectomy, to clean a blood vessel. Reproduced with permission from [114]. Copyright (2016) IPEM.

vessels as plaque is able to regress [109]. Statin therapy to lower low-density lipoproteins (LDL) concentration is a commonly used treatment to combat plaque buildup [110]. However, with the prevalence of additional conditions such as diabetes, obesity, or poor lifestyle choices, LDL concentrations may not always be controllable even with medication [111]. Extensive research with transgenic mice led to the postulation of an inverse relationship between blood coagulation and atherogenesis as hypercoagulability in mice typically increased atherosclerosis, and hypocoagulability reduced the atherosclerotic character [112]. The use of anticoagulants on humans have been less promising [113]. Surgical intervention is another possible treatment of

plaque buildup but is generally utilized when other medical options have been exhausted due to the associated trauma with the procedure and higher mortality rates in patients over the age of 70 [115]. Atherectomy is a procedure designed to remove plaque from blocked arteries; the most common procedures are generally directional, rotational, orbital, and laser atherectomies [116]. A directional atherectomy (DA) apparatus is comprised of a cup-shaped cutter nestled within a housing unit and a small balloon [117]. When a DA was utilized on the left main coronary artery, an evaluation of 101 patients determined that DA has acceptable low restenosis rate and high survival rates [118]. Rotational atherectomy (RA) is a niche technique utilized for heavily calcified or fibrotic and undilatable lesions, where balloon angioplasty is unusable [119]. The efficacy of RA procedures are high with relatively low risk of complications [120]. However, there are concerns that RA can cause distal embolization which is why an orbital atherectomy (OA) can also be used to clear heavily calcified plaques [121]. Further, randomized clinical testing is required to determine the efficiency of OA over RA [122]. Excimer Laser Coronary Atherectomy (ELCA) is intended to be a robust atherectomy procedure, but ELCA has less favorable outcomes with heavy calcification: 79% with calcified plaque versus 96% with non-calcified, meaning that RA/OA is still the desired method for heavily calcified plaque [123]. Even with the promising clinically practiced approaches summarized above, it is fair to say that strategies for removal of plaque have had limited success and there is significant room and an urgent need for improvement (Fig. 3).

5. A brief introduction to Active Matter

As discussed previously, active particles and systems are ubiquitous in nature: a flock of birds that show stunning collective behavior [124,125], spermatozoa that are attracted to the egg cell during fertilization or the synchronized ciliary swimming of the pond dwelling protist *Paramecium* [126]. Synthetic active matter at the microscale largely consists of self-propelled or externally propelled

particles which differ in their principle of operation. While both self and externally propelled nanomotors/swimmers derive their energy from the surroundings such as by chemical reactions or from external power sources, the direction of motion of externally propelled nanomotors is tied to the external power source [1,3,127]. In this review, we adopt a broad definition of active matter which includes both these classes of nanomotors. Active nanoparticles differ from Brownian nanoparticles in terms of enhanced transport properties, where the diffusivity of the active particles is significantly larger than to passive Brownian nanoparticles of the same size. Different power sources such as magnetic or ultrasound fields, catalytic reactants, and even energetic molecules such adenosine triphosphate (ATP) have been utilized to drive motion in active particles. Also, researchers have utilized active particles as delivery vehicles for drugs, genes and other biological molecules to cells or tumor spheroids [67,128–130], for separation of biomolecules/cells [131,132] and purification of oil water suspensions [133]. Recently, nanomotors have been investigated for active delivery of clarithromycin in the mouse stomach to treat H. pylori [18] via prolonged adhesion time in the stomach and intestines [18,69,134]. However, only a few of these particles are ready for clinical tests due to the lack of sufficiently high energy reserve or biocompatibility issues. In the sections below, we first take a look at the most important types of active particles developed, pertaining to their applicability towards tumor/tissue penetration as well as clot/plaque removal from blood vessels. We then briefly discuss their active transport properties and argue that they can overcome the biological forces that are encountered in a blood vessel or in the tumor microenvironment. For a more detailed description of the various methods used for the manipulation of these micro/nanomotors and their fabrication principles, the reader is directed to other detailed reviews [135–138].

5.1 Examples of active matter for enhanced transport

5.1.1 Active matter driven by chemical reactions

Fuel driven active matter systems are generally rod or tube shaped and coated with materials that can catalyze the decomposition of a chemical fuel, thus generating gaseous products such as hydrogen and propelling the system forward [139–141]. Another type of fuel driven active

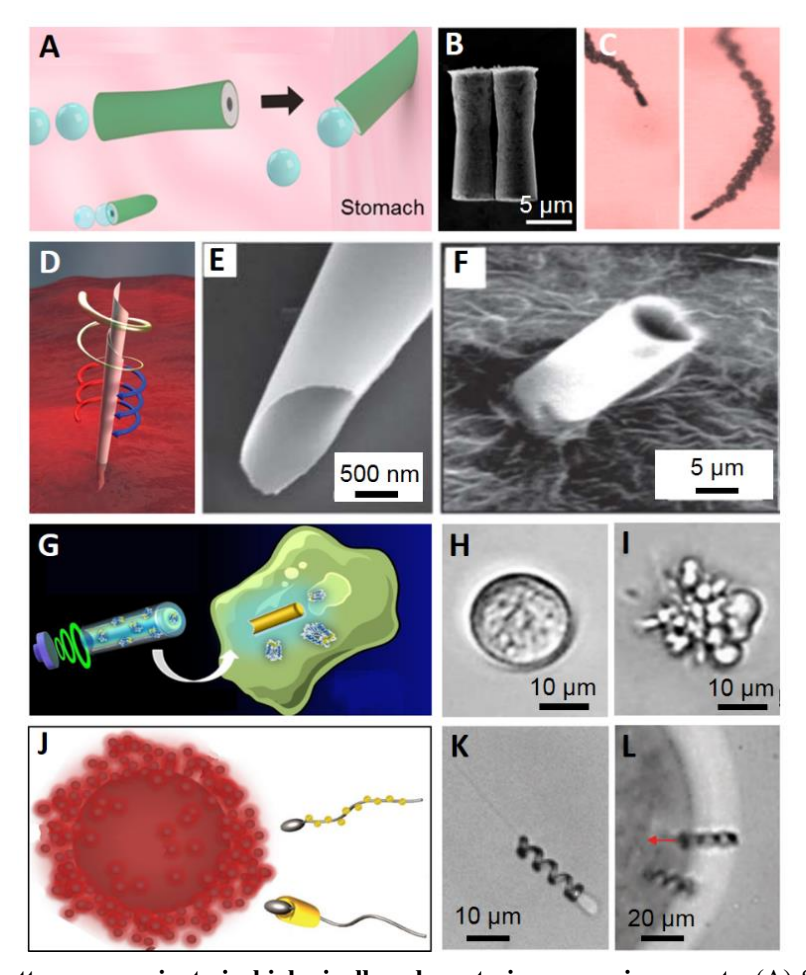


Fig. 4. Active matter can navigate in biologically relevant viscous environments. (A) Schematic of the in vivo propulsion and tissue penetration of zinc-based micromotors in stomach; (B) SEM image of zinc-based micromotors; (C) time lapse images of the propulsion of micromotors in gastric acid. Reproduced with permission from [134]. Copyright (2015), American Chemical Society. (D) Schematic of a rolled-up magnetic microdriller; (E) SEM image of a ferromagnetic rolled-up microtube with a sharp tip; (F)SEM of a microdriller embedded into a pig liver section after drilling. Reproduced with permission from [140]. Copyright (2013), the Royal Society of Chemistry. (G) Schematic of nanomotor-based intracellular delivery of an enzyme to induce apoptosis of the recipient cell; (H) time-lapse images of a healthy human gastric adenocarcinoma (AGS)cell, and (I) an apoptotic AGS cell after nanomotor delivery. Reproduced with permission from [129]. Copyright (2017), American Chemical Society. (J) Schematic of sperm cell-based hybrid microswimmers targeting an oocyte. (K) Optical microscope image of a helical microswimmer that is carrying a bovine sperm cell. (L) Transport of an immotile sperm from a microhelix onto the oocyte wall. Reproduced with permission from [150]. Copyright (2017) Wiley-VCH.

matter contains a galvanic cell that creates a local gradient of ionic concentrations [6,142]; as a result, the motor moves due to an electrophoretic force. The most widely used fuel has been hydrogen peroxide together with a platinum catalyst deposited on the nanomotor [143]. However, the high concentration of peroxide needed for operation can be toxic and hence makes peroxide based nanomotors unsuitable for *in vivo* applications. Motors that work on other fuels such as magnesium-based motors which move in water [144, 145], or zinc-based motors which self-propel in acidic environments, as found in the stomach [146, 147], are potentially applicable *in vivo* and are shown in **Fig. 4**A-C [144,146]. Enzymatically propelled motors are also promising for improved biocompatibility but the speeds and forces generated are smaller than bubble propelled motors [128,147,149].

Fuel driven active matter has been shown to reach speeds of hundreds of µm/s to mm/s [151,152, 153] and can generate forces suitable to penetrate tissue/cell membrane [140]. Though these types of nanomotors have been demonstrated to be useful for *in vivo* drug delivery in the mouse stomach and intestine [154,155] and also for live animal imaging [69], their transport characteristics in complex heterogeneous media like tissues has not yet been explored. Problems such as effectively replenishing the reactants or the limited number of biocompatible reactions remain unsolved.

5.1.2 Magnetically driven active matter

Magnetically driven nano/micromotors have also been widely explored over the last decade, particularly due to the inherent biocompatible nature of the driving force. Magnetic microdaggers could be navigated *in vitro* using rotating magnetic fields, towards cancerous HeLa cells delivering the anti-cancer drug Camptothecin. Interestingly, the drill like motion of the microdaggers could generate enough force to pierce into the cell membrane leading to cell death

[156]. Helical nanomotors have been fabricated [157–159] and navigated with very small magnetic fields in viscous and complex environments like glycerol [160], human blood [161], hyaluronic acid [162], mucin gels [163], the intracellular environment [66], as well as the vitreous humor of the eye [164]. Generally, magnetically driven nanomotors all move in the same direction decided by the magnetic field. However, recent research has shown that it is possible to decouple the orientation of the nanomotors by only providing energy to the motors [165] such that the motion of different nanomotors can be controlled in an independent manner [127,166]. Magnetically driven nanomotors hold great promise because of their ease of miniaturization and navigability in an environmentally independent manner. As shown in **Fig. 4**D-F, magnetically driven microdrillers were able to penetrate into a section of pig liver. However, apart from a few preliminary studies [167,168], successful navigation of these nano/micromotors in *in vivo* environments are yet to be demonstrated.

5.1.3 Acoustically driven active particles

Ultrasound has been widely used in clinical settings and hence is a suitable source of energy for the propulsion of nano/micromotors in biologically relevant media such as serum, PBS, saliva and the intracellular environment [169]. When micro/nanoparticles in a liquid are placed in close proximity to an ultrasonic transducer, the particles are levitated to the high-pressure nodes of the acoustic waves and show translational motion in the plane [170]. Various kinds of motion like high speed rotation and chain formation have been observed, and the speed of motion can reach several hundreds of µm/s [171,172]. The motion was also found to be sensitive to the shape asymmetry along the length of the particles. **Fig 4** G-I demonstrate how ultrasound driven nanorods can be used for intracellular delivery of enzyme to induce apoptosis of the recipient cell. Ultrasound can also be used to drive nano/micromotors based on acoustic droplet vaporization at

a staggering speed of 6 m/s [173]. The limitations of acoustically driven nanomotors for biomedical applications include geometry dependent motion and high-power requirements.

5.1.4 Bio Hybrid active matter

To further improve the power efficiency of micro/nanomotors, bioinspired approaches are being explored [174–177]. Biological cells such as muscle cells [178,179] or bacterial cells [180] can generate mechanical forces and torques by harnessing energy from the surrounding environment [181]. For instance, tumor associated monocytes (TAMs) which are produced as the body's response to the malignancy of a tumor, can migrate to the less accessible tumor hypoxic regions, and be used to deliver therapeutics to the interior of a tumor [182,183].

Bacterial powered motors have been used to deliver proteins inside cells and organs such as the kidney and intestine in a mouse model [184–186]. Magnetic nanoparticles can be internalized by the bacteria, and used to provide motion orientation by external magnetic fields [187]. Spermatozoa driven micromotors are an exciting new concept in which rolled up microtubes or other synthetic constructs are used to capture sperm cells causing them to self-propel [67]. Such systems have been explored for applications including artificial fertilization (**Fig. 4** J-L) and drug delivery to HeLa cell spheroids [148,188].

5.2 Transport properties of active matter

We see above that different types of active particles have been developed with several built-in functionalities. In this section, we take a look at their transport properties, particularly from the perspective of motion inside the tumor microenvironment. We also estimate the forces that these particles can generate and compare them to the forces required to penetrate plaques or tissues.

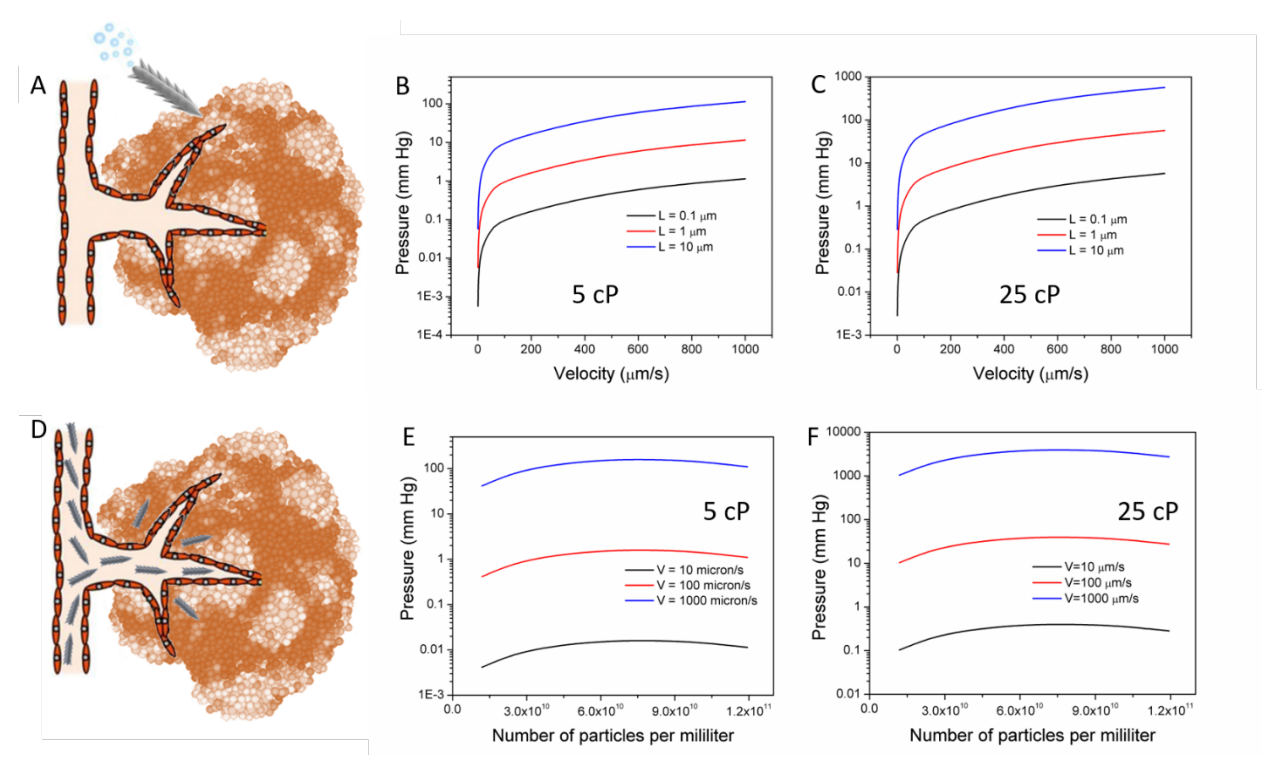


Fig. 5. Enhanced transport properties of active particles. (A) Drag based thrust exerted by a single active particle. This thrust is also a function of the speed and the size of the particle. The drag-based thrust is plotted for two different viscosities, (B) 5 cP and (C) 25 cP. For plots in panels B and C, we have assumed a cylindrical particle whose length is equal to the diameter and has a pointed tip, 100 nm in radius. (D) A swarm of active particles can exert pressure to enter the tumor stroma. This active pressure is dependent on the speed of the active particles, their concentration as well as the viscosity of the surroundings. Active pressure plotted for different speeds at viscosity, (E) 5cP and (F) 25 cP. For plots in panels E and F we have assumed an ensemble of spherical particles of radius 1 μm.

Metastatic breast cancer cells in human primary tumors use ECM fibers as guides to reach the blood vessels through the dense tumor stroma [189]. The motion is believed to be chemoattractant in nature. These cells also create blebs and can degrade and reorganize the ECM fibers as and when required. Cancer cells are squishy, and that helps them to successfully reach the bloodstream by crossing the endothelial cell barrier of the vessels [189–191]. Migration of cancer cells represents a gold standard that researchers could look towards to achieve efficient transport through the tumor microenvironment. In contrast, conventional nanotherapeutics can only passively migrate through the tumor stroma without altering the fibers. Present day active particles are also significantly less efficient at migration as compared to metastatic cancer cells. Yet, they show enhanced transportation properties when compared to the passive nanotherapeutics

while moving through the interstitial spaces, and as we argue below, active particles can also generate enough force to penetrate through the fibrous network in the tumor ECM.

The motion of passive Brownian particles is governed by the random collisions with the surrounding molecules and comes under the purview of equilibrium thermodynamics (Gaussian) equations. In a Newtonian fluid, the mean square displacement of an incompressible spherical passive Brownian particle is given by $r^2 = 6Dt$, where $D = \frac{k_B T}{6\pi u a}$ is the diffusion coefficient of the particle, T is the equilibrium temperature; a, the characteristic radius of the particle; μ , the viscosity of the surrounding medium; t, the time and k_B , the Boltzmann constant. Active particles, on the other hand, derive their energy from the surroundings and can convert them in a directed motion. The motion of active particles can be defined [192] by the random Gaussian fluctuations described above in addition to a characteristic velocity v. In a simplified 1-D model, the mean displacement can be written as, $\langle x(t) \rangle = v \tau_r \left[1 - e^{-\frac{t}{\tau_r}} \right]$. We see from the equation that on a short time scale $(t \ll \tau_r)$, the motion is directed with a velocity v, while it becomes super diffusive at a time scale much larger than the rotational diffusion time τ_r , which essentially means a more extensive coverage of space by the active particles. Thus, an active particle can show significantly more net displacement at time scales greater than τ_r (the typical value of τ_r is of the order of seconds for a 1 µm spherical particle) as compared to a passive Brownian particle [192]. We note that unicellular organisms like E.coli, use a similar idea to move faster than what they could by mere diffusion. In this case, the bacterium derives its energy to move by flagellar motion derived from ATP hydrolysis, and it alters between fluctuating run and tumble motions, where the run phase is chemoattractant in nature [193].

The motion of active particles in a heterogeneous medium is however of particular concern for assessing applicability in vivo. Though the theory of Brownian motion in heterogeneous media is more or less well understood [194], the same is not true for active particle transport in heterogeneous media, barring a few numerical models. It was shown that for randomly positioned hard obstacles, active particles could demonstrate either diffusive or sub diffusive behavior depending on the reorientation speed of the particle after encountering an obstacle [195]. Also, the two most common swimming strategies at low Reynolds number, namely the flexible oar-like motion and the helical corkscrew-like motion showed an enhanced speed when put in a simple two-phase system containing hard obstacles dispersed in a Newtonian fluid [196]. Researchers considered a more realistic model [197], comprised of a compliant network such that the fluid flow created by the active swimmers could cause elastic changes to the surrounding mesh which could also interact with the surrounding viscous fluid. In this case, the swimming of active flagellar elements could cause enhanced swimming speeds for stiffer network filaments. Experiments show similar speed enhancements of E. coli bacteria in methylcellulose gel [198]. The authors argued that the gel network helped to reduce the hydrodynamic circumferential slip of the thin bacterial flagella in the fluid, similar to the motion of a corkscrew through hard materials. The results, however, strongly depended on the size of the bacterial flagella relative to the pore size in the gel [162]. Indeed, larger helices in viscoelastic media were found to show both an increase and decrease in speed compared to viscous fluids [199,200], depending on the fluid elasticity and speed of rotation of the helix (Deborah number) [201]. Further experimental and theoretical work is required to extend our understanding of the motion of active particles in heterogeneous media. Further modifications are also needed to understand the effects of confinement [202]. For example, as discussed in the previous sections, the surface electric charge of the particles plays a significant

role in transport through biological media, and its effect on the motion of active particles is still unclear.

We now estimate the force F generated by a single active particle (Fig. 5A). The motion of particles at the nano/microscale is governed by low Reynolds number hydrodynamics, where the Navier Stokes equation is reduced to the linear Stokes equation, where the pressure p, and velocity v is related to the applied force f by $\nabla p - \mu \nabla^2 v = f$, which does not contain any inertial term and μ is the dynamic viscosity. In the Stokes' flow regime, the motion of the particles is highly dissipative, and they will come to a stop as soon as the applied energy/force f is withdrawn [203–205]. The drag force that the particle experiences is given by $f_{drag} = -\mu Gv$, where G is the geometric drag coefficient. Due to the absence of inertial effects, the force that the particle exerts in the direction of v is $-f_{drag}$. This drag based thrust is thus dictated by the velocity of propulsion of the active particle, which in turn is strongly dependent on the actual principle of motion. For example, the speed of a spermatozoa has been predicted by resistive force theory [206] to be $v_{sperm} = \frac{2f_{beat}\pi^2b^2}{\lambda} \left[\frac{1}{1+\frac{4\pi^2b^2}{\lambda^2}}\right]$, while the velocity of a helical magnetic nanopropeller [207] is given by $v_{propeller} \approx \Theta\Omega[(\xi_{\perp} - \xi_{\parallel})\xi_r^h]/[\xi_{\perp}\xi_{\parallel}R_h]$. We see that the velocity for the sperm like or helical swimmers are dictated by parameters like the beating frequency f_{beat} , and the rotation frequency of the magnetic field Ω and other geometrical parameters like the width of the flagellum b, the wavelength of the flagellum λ , the parallel (ξ_{\parallel}) and perpendicular (ξ_{\perp}) geometrical drag coefficients of the flagellum, radius of the head R_h and the pitch angle Θ . On the other hand, the velocity of an active catalytically powered nanorod [6] is given by $v_{catalytic} =$ $\frac{SR^2\gamma}{2\mu DL[H_2O]} ln\left(\frac{L}{2R}\right) \left[ln\left(\frac{2L}{R}\right) - 0.72\right]$, where the velocity is dependent on the reaction rate S, and the interfacial surface tension γ and the geometrical parameters like the length L and the radius R of

the rod and the Brownian diffusion coefficient D. Apart from the velocity, the thrust is also dependent on the viscosity and the drag coefficient of the particle. Larger particles usually have larger drag coefficients and can thus produce a larger thrust for the same velocity. It is, however, noteworthy that active particle systems are usually not very energy efficient [208], because of the large amount of dissipation associated with their motion. Thus, increasing the force by using a larger particle might not be easy. For example, the energy conversion efficiency is only of the order of 10⁻⁹ for self-electrophoretic/diffusiophoretic swimmers, around 10⁻⁷ for acoustically powered motors and around 10⁻² for magnetic helices. In constant velocity systems like the magnetically driven helices, the energy required to drive the system can increase or decrease depending on the viscosity of the surroundings and hence a range of thrusts can be produced by driving these particles in increasingly viscous environments [160]. A calculation of the forces exerted shows that in a medium of viscosity of 5 cP, similar to interstitial fluid, a 10 µm long active particle can generate a pressure of 10 mm Hg while moving at a speed of 100 µm/s (Fig. 5B). A similar comparison of the forces caused by particles of different dimensions is plotted for two different viscosities (Fig. 5B, C). It is worth noting that the IFP inside a tumor is of similar orders of magnitude [105], which shows that the active particles can be strong enough to overcome the IFP while extravasating in the tumor stroma.

Another way of looking at the pressure exerted by active particles is at an ensemble scale (**Fig. 5D**). While individual active particles can locally exert pressure to overcome the opposing forces, a swarm of active nanomotors can exert a collective *active pressure* on their surroundings [209–211]. This pressure is similar to the pressure exerted by the molecules of a gas or a liquid on the container in which it is stored. Calculations show that the active pressure of particles can be as high as 1 Pa, for a spherical particle of diameter 1 μ m, moving at a speed of 10 μ m/s in a 10%

suspension. While detailed calculations based on phenomenological models of active particles have been carried out, this hypothesis was experimentally verified where the pressure exerted by active particles was measured using an acoustic trapping technique [5]. Thus, a swarm of nanomotors can potentially overcome biological barriers like the IFP in the tumor ECM. To compare the values, we have plotted the active pressure of particles moving at different speeds and

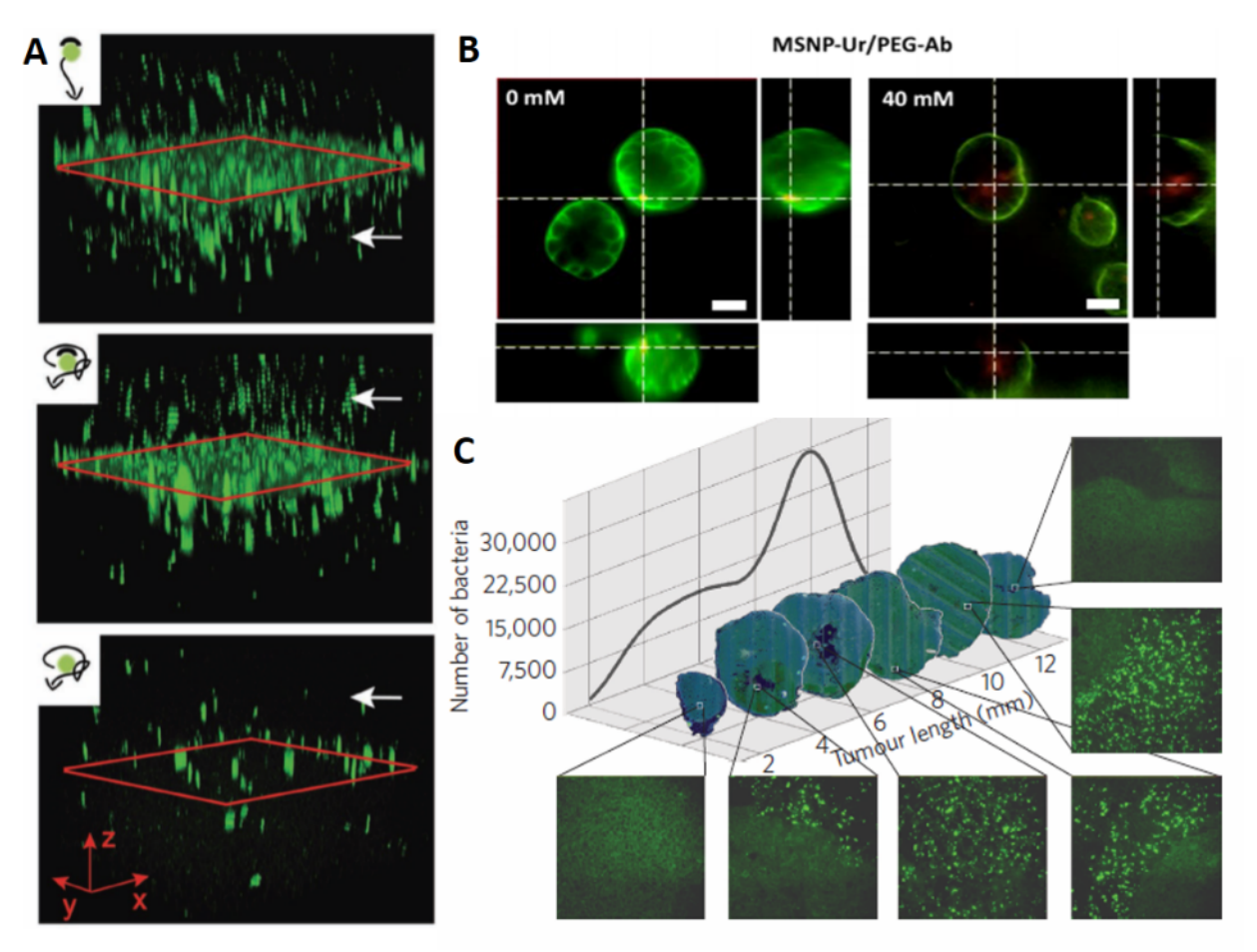


Fig. 6. Active particles can enhance permeation through tumor spheroids. (A) (top panel) The fluorescent Janus motor distribution for the Janus motor/H2O2group, the white arrow points to the particle enriched bottom chamber, the particle ratio of top chamber/bottom chamber is 1:1.39; (middle panel) fluorescent Janus motor distribution for the Janus motor/H2O control group, the white arrow points to the particle enriched top chamber, the particle ratio of top chamber/bottom chamber is 2.51:1; (bottom panel) fluorescent polymersome control distribution for the non-motor/H2O2group, the white arrow points to the particle enriched top chamber, the particle ratio of top chamber/bottom chamber is 2.46:1, x and y axes are 580 _m in length and z axis is 400 _m in height. Reproduced with permission from [212]. Copyright (2018) Wiley-VCH. (B)Fluorescence images of mesoporous silica nanomotors powered by urease incubated with tumor spheroids having 0 mM and 40 mM urea, showing that the nanomotors can enter the tumor spheroids. Reproduced with permission from [128]. Copyright (2018) American Chemical Society. (C) Transverse tumor sections of MC-1–LP after targeting. Images of each section were acquired using a fluorescence optical microscope equipped with a ×40 magnification objective lens. The images show a good distribution of the loaded MC-1 cells throughout the tumor. Reproduced with permission from [186]. Copyright (2016) Macmillan publishers limited.

of various sizes as a function of the number of particles per unit volume (**Fig. 5**E, F). For example, the IFP in a tumor is around 10 mm Hg [105], which is comparable to the pressure generated by 1 μm active particles moving at speeds of 100 μm/s (**Fig. 5**F) in a viscosity of 25 cP.

5.3 Examples of active particle systems for tumor penetration and clot removal

Here, we discuss three specific cases where enhanced transport has been demonstrated in a tumor or a tumor vasculature model. In the first example, the researchers investigated the motion of platinum sputtered polymersomes across a leaky tumor vasculature model [212]. The researchers used a porous silicon oxide membrane with 8 µm pores scattered throughout the membrane to replicate the gaps in a leaky tumor vasculature separating two chambers. The membrane was further seeded with endothelial cells. The active polymersome particles were found to show enhanced diffusion (Fig. 6A) under the influence of hydrogen peroxide across the vasculature model membrane compared to the control groups that do not have peroxide. In another example [128], researchers used urease powered active particles to demonstrate increased diffusion into spheroids made of bladder cancer cells. The particles were functionalized by polyethylene glycol and antibodies to target the cancer cells. The particles showed enhanced diffusion in the presence of urea which is found in large quantities in the urinary bladder. After four hours of incubation with the urease powered particles, the tumor spheroids were progressively less viable with higher concentrations of urea. It was also found that the particles could be successfully internalized inside the spheroids in the presence of urea and the internalization efficiency was increased up to 4 times with the cell targeting antibodies (Fig. 6B). In another seminal study [186], magneto aerotactic bacteria were loaded with drug containing nanoliposomes and guided to the hypoxic regions in the tumor in a live mouse. The MC-1 bacteria used in this study show a natural tendency to move towards oxygen deficient regions. Further, these bacteria contain chains of magnetic particles

called magnetosomes that can be exploited to guide them to the tumor interior by providing a small orienting torque that helps to overcome the Brownian rotational diffusion. It was found that almost 55% of the drug loaded bacteria could enter the tumor interior and the number of bacteria was found to increase towards the center of the tumor xenograft (**Fig. 6**C).

The other clinical problem we discuss concerns the eradication of plaque from blood vessels which is one of the major techniques in the treatment of heart disease. While conventional atherectomy procedures can perform this task, complications can arise due to unwanted bleeding and damage. Active particles could potentially offer a less invasive method of blood clot/plaque removal by mechanical rubbing of the clot [213–215]. Below, we present a few recent studies which have shown the capability of these systems to perform this procedure. Helical magnetic particles (**Fig. 7A**), having a length of a few mm, were guided using a rotating magnetic field and localized using ultrasound feedback inside an *in vitro* model of a blood vessel [216]. The model used a catheter containing a blood clot and PBS was flowed through the catheter at speeds similar to that found in blood vessels of similar diameter. The magnetic helical particles were shown to grind through the blood clot by breaking the fibrin network (**Fig. 7B**). A similar principle was used in another class of biohybrid helicoids containing iron oxide nanoparticles in a 3D printed scaffold [217]. The helicoid particles were used to drill through biofilm occluded paths in an *in vitro* model (**Fig. 7C**).

We envision that using micro/nanoscale active matter to directly interact and remove plaque is a promising approach as well (**Fig. 7**D and E). For this purpose, microparticles with spiky structures or 'hedgehog' particles have significant advantages over conventional regular shaped particles for several reasons [218]. First, spiky microparticles do not interpenetrate each other with their spikes, which significantly reduces the contact area and attractive forces between them, thus preventing

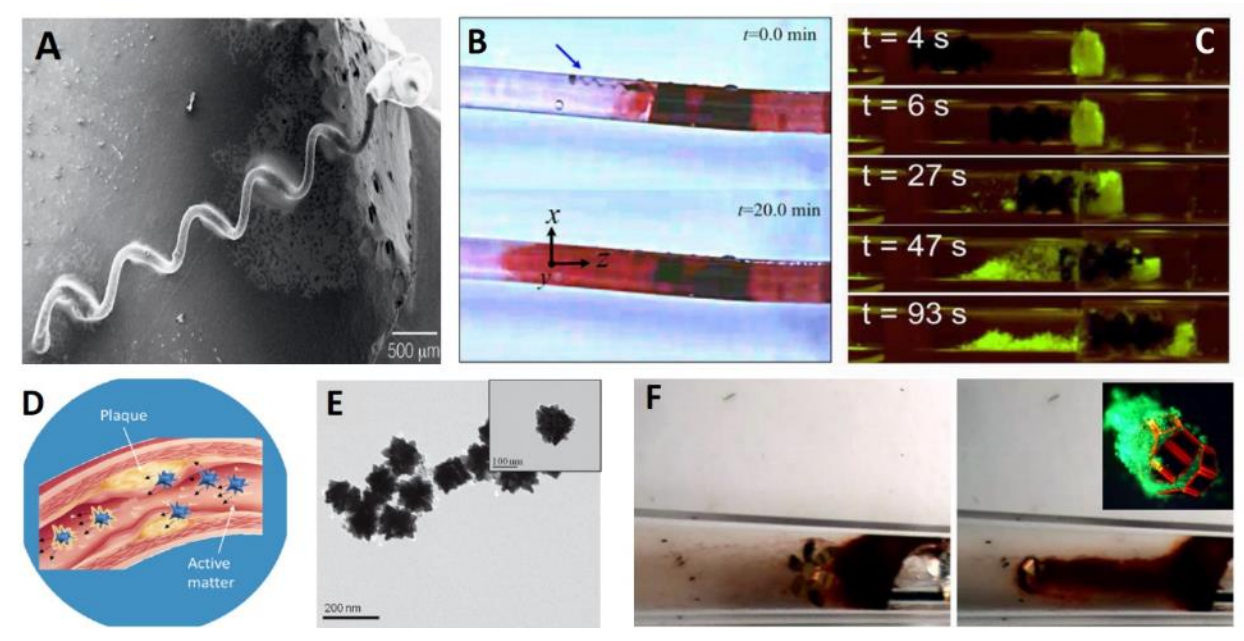


Fig. 7. Abrasive particles can help remove plaque from blood vessels. (A) A helical microrobot proposed for clearing up blood clots. Reproduced with permission from [216]. Copyright (2018) IEEE. (B) The microrobot can help clear up blood clots by cutting through the fibrin network when subjected to a rotating magnetic field. Reprinted with permission from [241]. Copyright (2016) IEEE. (C) Helicoid catalytic antimicrobial robots (CARs) could also drill and restore biofilm-occluded paths. Fluorescent images showing the action and biofilm removal efficacy of helicoid robots: green color indicates *S. mutans* biofilms or clogs. Reproduced with permission from [217]. Copyright (2019) The Authors. (D) Conceptual schematic showing that a slurry of abrasive active microparticles can be used to clear up clots and plaque build-up in the blood vessels. Image background credit: Intermountain Healthcare Heart Institute. (E) An example of gold coated magnetic supraparticles. Reproduced with permission from [220]. Copyright (2013) Wiley-VCH. (F) Magnetically guided microgrippers can remove biopsy samples from a piece of porcine liver. In a similar manner, they can be engineered to remove clots from blood vessels. (Inset) A clump of viable cells after biopsy by the microgrippers. Reproduced with permission from [221]. Copyright (2009) The National Academy of Sciences.

aggregation in the bloodstream [219]. Second, conventional micro/nanoparticles necessitate the use of surfactants or ligands on the surface to prevent aggregation, but the surfactants can significantly reduce the surface hydrophobicity and decrease their interaction with hydrophobic plaque [222]. Third, the spiky microparticles can be extremely oleophilic *via* surface functionalization to enhance their penetration into the plaque. If the spiky microparticles have magnetic components inside, their motion and collection can be further controlled using the magnetic field. It has been demonstrated that such spiky microparticles can be used for efficient oil emulsion cleaning and oil—water separation [223]. It would be interesting to see whether the spiky or corrugated particles can be rendered active and whether they can be used for removal of

plaque in blood vessels. Untethered shape changing microgrippers (**Fig. 7**F) [220] which can be guided through the blood vessels by an active propulsion technique to the desired location could be made to actuate and tear away the plaque. Such systems have already been used for tissue excision in the biliary tree of a pig [70,71].

6. Discussion and outlook

In summary, conventional nanoparticle drug delivery strategies are limited by transport to cancer cells inside tumors. Nanoparticles, both passive and targeted, have limited penetration into the cancer stroma away from the blood vessels [14]. Hence, techniques that improve the nanoparticle diffusion inside the tumor extracellular matrix are required. Micro/nanomotors, discussed in the previous sections can be useful in this regard, as they show significantly higher diffusion due to the energy delivered from external power sources or harnessed from the surrounding environment. The key functional improvements for this class of therapeutic particles to achieve transport in the tumor microenvironment or to remove plaque in blood vessels can be listed as follows:

a) Sustained source of energy: It is essential to have sustained motion for a few hours inside the tumor in order to populate and deliver therapeutics to all the cancer cells. Until now, the duration of motion for catalytic and bubble propelled nanomotors has been rather limited because of rapid reaction rates with the medium. The fuel lifetime can be significantly increased by using larger particles which are tens of microns in size and where the active material is encapsulated, resulting in controlled use of the fuel. These larger particles may need to be precisely structured at smaller length scales so that the lifetime of motion can be increased significantly to several hours, or even days. Polymersome nanomotors could be useful in this regard, albeit the use of hydrogen peroxide and platinum chemistry limits applicability in vivo. Magnetic or ultrasound propelled

nanomotors, that are externally driven offer advantages in this regard due to a continuous source of energy that can be delivered over prolonged time periods. For these systems, it is important to find more efficient ways of transferring the energy to the tumor workspace. These motors can be activated only when the particles reach the tumor site through the bloodstream. Also translation to a clinical scenario is the biggest challenge of these systems where human-sized magnetic coils and ultrasound transducers may be required to enable operation within large animals and humans. Alternatively, smaller magnetic and ultrasound instrumentation that could be used locally on different parts of the human body are also appealing. Biohybrid motors are also very promising in this regard, however, their engineering can be difficult and the potential risk of infection remains.

- b) Ability to move in swarms: As discussed above, in order to generate sufficient pressure to overcome the interstitial pressure, micro/nanomotors have to be present in large numbers. This requires swarm movement capabilities in which potentially billions of nanomotors can be moved together in the tumor workspace. While the transport of the nanomotors to the tumor blood vessels will be mainly governed by the blood flow characteristics, the nanomotors working in large numbers can overcome the physical and chemical barriers inside the tumor stroma. There are associated challenges in moving large numbers of microscopic motors without aggregation; clumping would significantly increase their size and impede functionality.
- c) Higher speeds in terms of body lengths/sec: Higher speeds of motion are essential to generate sufficient forces to overcome the barriers inside a tumor. By far the fastest nanomotors have been the ultrasound and the bubble propelled motors with speeds upto several hundreds of µm/s to mm/s [153]. Additional studies are needed to optimize shape, surface composition and chemistry for highly efficient energy conversion and motion.

- d) Ability to move in biologically relevant media: Magnetic nanomotors have been shown to exhibit motion in media such as hyaluronan gel and the cellular cytoplasm. Nanomotors that are larger than 1 µm were unable to penetrate hyaluronic gel, while 500 nm long motors could penetrate them because of increased diffusion [162]. The same group also showed the ability to penetrate mucin gels by functionalization of the nanomotors with mucus dissolving chemicals [163]. Recently [66], magnetic nanomotors have been successfully navigated inside live cells with micrometer scale precision and also in undiluted human blood by coating the nanomotors with cytocompatible coatings of iron ferrite [161]. Similarly, researchers were able to show the navigation of acoustically driven nanomotors inside live cells. Thus, externally driven nanomotors show great promise for propulsion in the tumor microenvironment, but motion in this heterogeneous environment and also through and across other biological barriers needs to be investigated.
- e) Large scale fabrication techniques: As discussed above, it has been estimated that less than 2% of the particles manage to reach the tumor through the bloodstream. Thus, huge numbers of nanomotors will be required to result in any useful fraction reaching the tumor interior. Bottom up synthesis methods or high-throughput 3D microfabrication methods will be needed to generate the large numbers of motors per batch of fabrication. For example, for an injected dose of 10¹⁰ number of nanomotors in the bloodstream, we anticipate that only on the order of 10⁸ nanomotors will be able to reach the tumor site. To put these numbers in perspective from a fabrication standpoint, glancing angle deposition (GLAD), which is a 3D physical vapor deposition technique, can produce up to 10⁹ nanomotors in a single fabrication step on a 4" wafer [157].
- f) Biocompatibility and bioavailability: While catalytic nanomotors have been shown to be multifunctional, a big concern in the field is the choice of materials. Many motors investigated in

the laboratory are composed of materials that are toxic or utilize chemical environments that are not present in the human body. For example, the concentrations needed in the hydrogen peroxide fuel system are not well suited for *in vivo* experiments. Also, ensuring eventual clearance from the body or biodegradability of the motors upon completion of their task is a big concern [224] as it is going to be virtually impossible to retrieve all of the nanomotors. This concern is especially acute if the motors are deployed intravenously, which raises the potential for transient or permanent blockages due to accumulation or aggregation. Very little research has been done to address these concerns, and the field of dissolvable microrobots has only recently started gaining traction [225,226].

Another concern is the bioavailability of nanomotors inside the tumor as most of the particles are usually cleared by the immune system of the body and alternate strategies to circumvent immune clearance need to be discovered. Techniques like pegylation have improved the circulation time of nanoparticle drug depots in blood [227,228]. Cell encapsulated nanomotors might also be pertinent in this regard where nanomotors can be circulated in a stealth fashion [229] and their cover would be removed once the motor reaches the tumor site.

g) Advanced imaging techniques: The development of the field is closely tied to the adoption of advanced molecular imaging and spectroscopic techniques for tracking and targeting of the active particles in live animals [69,168]. Bioluminescence and infrared imaging can be beneficial for superficial organs and for imaging in small animals [230,231]. Contrast agents like carbon nanotubes for example, can significantly improve the visulaization of the active particles when used in conjunction with photoacoustic (PA) and photothermal (PT) imaging [232]. However, for tumors located deep in the body, positron emission tomography (PET), computed tomography (CT) or radiolabeled magnetic resonance imaging (MRI) are required [233,234].

Needless to say, there are many hurdles that need to be overcome in Active Matter Therapeutics. But we do not anticipate that any of these concerns are insurmountable. Many challenges could be overcome by investigating strategies to augment conventional nanoparticle approaches with activity and motion. For example, recent adoptions of mesoporous silica nanoparticles for fabricating nanomotors have opened up new possibilities pertinent to the drug loading abilities of active particles [235-238]. Indeed, recent literature provides examples where several of the previously mentioned challenges are being addressed [239,240] and it is also clear there is an urgent need to more widely investigate active matter to overcome critical bottlenecks in modern therapeutics.

Acknowledgements

We acknowledge support by the National Institute of Biomedical Imaging and Bioengineering of the National Institutes of Health under Award Number R01EB017742. The content is solely the responsibility of the authors and does not necessarily represent the official views of the National Institutes of Health. We also acknowledge support from the National Science Foundation (EFMA-1830893).

References

- [1] S. Ramaswamy, Annu. Rev. of Condensed Matter Phys. 1 (2010) 323–345.
- [2] I. Prigogine, I. Stengers, Order Out of Chaos: Man's New Dialogue with Nature, Verso Books, 2018.
- [3] M.C. Marchetti, J.F. Joanny, S. Ramaswamy, T.B. Liverpool, J. Prost, M. Rao, et. al., Rev. Mod. Phys., 85 (2013) 1143–1189.
- [4] V. Narayan, S. Ramaswamy, N. Menon, Science. 317 (2007) 105–108.
- [5] S.C. Takatori, R. De Dier, J. Vermant, J.F. Brady, Nat. Commun. 7 (2016) 10694.
- [6] W.F. Paxton, K.C. Kistler, C.C. Olmeda, A. Sen, S.K. St Angelo, Y. Cao, et. al., J. Am. Chem. Soc. 126 (2004) 13424–13431.
- [7] G.M. Whitesides, B. Grzybowski, Science, 295 (2002) 2418–2421.
- [8] Y. Xia, Y. Xiong, B. Lim, S.E. Skrabalak, Angew. Chem. Int. Ed Engl. 48 (2009) 60–103.
- [9] L.A. Austin, B. Kang, M.A. El-Sayed, Nano Today. 10 (2015) 542–558.
- [10] P.-C. Chen, X. Liu, J.L. Hedrick, Z. Xie, S. Wang, Q.-Y. Lin, et. al., Science, 352 (2016) 1565–1569.
- [11] J. Yan, M. Han, J. Zhang, C. Xu, E. Luijten, S. Granick, Nat. Mater. 15 (2016) 1095–1099.
- [12] T. Sanchez, D.T.N. Chen, S.J. DeCamp, M. Heymann, Z. Dogic, Nature, 491 (2012) 431–434.
- [13] A. Bricard, J.-B. Caussin, N. Desreumaux, O. Dauchot, D. Bartolo, Nature, 503 (2013) 95–98.
- [14] J. Palacci, S. Sacanna, A.P. Steinberg, D.J. Pine, P.M. Chaikin, Science, 339 (2013) 936–940.
- [15] W. Wang, W. Duan, S. Ahmed, A. Sen, T.E. Mallouk, Acc. Chem. Res. 48 (2015) 1938–1946.
- [16] M. Rubenstein, A. Cornejo, R. Nagpal, Science, 345 (2014) 795–799.
- [17] R. Fernandes, D.H. Gracias, Adv. Drug Deliv. Rev. 64 (2012) 1579–1589.
- [18] B.E.-F. de Ávila, P. Angsantikul, J. Li, M. Angel Lopez-Ramirez, D.E. Ramírez-Herrera, S. Thamphiwatana, et. al., Nat. Commun. 8 (2017) 272.
- [19] M. Medina-Sánchez, H. Xu, O.G. Schmidt, Ther. Deliv. 9 (2018) 303-316.
- [20] E. Blanco, H. Shen, M. Ferrari, Nat. Biotechnol. 33 (2015) 941–951.
- [21] G.P. Carino, E. Mathiowitz, Adv. Drug Deliv. Rev. 35 (1999) 249–257.
- [22] W.M. Pardridge, J. Cereb. Blood Flow Metab. 32 (2012) 1959–1972.
- [23] S.A. Liddelow, Fluids Barriers CNS. 8 (2011) 2.
- [24] L.M. Ensign, R. Cone, J. Hanes, Adv. Drug Deliv. Rev. 64 (2012) 557–570.
- [25] M.E.V. Johansson, H. Sjövall, G.C. Hansson, Nat. Rev. Gastroenterol. Hepatol. 10 (2013) 352–361.
- [26] N. Bertrand, J.-C. Leroux, J. Control. Release. 161 (2012) 152–163.
- [27] B. Olsson, E. Bondesson, L. Borgström, S. Edsbäcker, S. Eirefelt, K. Ekelund, et. al., Pulmonary Drug Metabolism, Clearance, and Absorption. In: Smyth H., Hickey A. (Eds.) Controlled Pulmonary Drug Delivery. Adv. in Deliv. Sci. and Technol. Springer, New York, 2011, pp. 21–50.
- [28] K. Park, J. Control. Release, 190 (2014) 3-8.
- [29] Y.H. Yun, B.K. Lee, K. Park, J. Control. Release. 219 (2015) 2-7.
- [30] V-R. María, F. Balas, D. Arcos. Angew. Chem. Int. Ed. 46 (2007) 7548-7558.
- [31] Y. Wang, Q. Zhao, N. Han, L. Bai, J. Li, J. Liu, et al. Nanomedicine 11, (2015) 313-327.
- [32] J.A. Hubbell, A. Chilkoti, Science, 337 (2012) 303–305.
- [33] N.A. Peppas, D.S. Van Blarcom, J. Control. Release. 240 (2016) 142–150.
- [34] J. Li, D.J. Mooney, Nat Rev Mater. 1 (2016) 16071.
- [35] H.R. Culver, J.R. Clegg, N.A. Peppas, Acc. Chem. Res. 50 (2017) 170–178.
- [36] S. Mura, J. Nicolas, P. Couvreur, Nat. Mater. 12 (2013) 991–1003.
- [37] M.W. Tibbitt, J.E. Dahlman, R. Langer, J. Am. Chem. Soc. 138 (2016) 704–717.
- [38] A. Gabizon, H. Shmeeda, Y. Barenholz, Clin. Pharmacokinet. 42 (2003) 419–436.
- [39] A.N. Lukyanov, T.A. Elbayoumi, A.R. Chakilam, V.P. Torchilin, J. Control. Release. 100 (2004) 135–144.
- [40] N.A. Peppas, J.Z. Hilt, A. Khademhosseini, R. Langer, Adv. Mater. 18 (2006) 1345–1360.
- [41] S. Merino, C. Martín, K. Kostarelos, M. Prato, E. Vázquez, ACS Nano. 9 (2015) 4686–4697.
- [42] H.M. Creque, R. Langer, J. Folkman, Diabetes. 29 (1980) 37–40.
- [43] V.A. Place, B.B. Pharriss, J. Reprod. Med. 13 (1974) 66–68.
- [44] K. Ishihara, K. Matsui, J. Polym. Sci. C 24 (1986) 413-417.
- [45] H. Maeda, H. Nakamura, J. Fang, Adv. Drug Deliv. Rev. 65 (2013) 71–79.
- [46] A. Banerjee, J. Qi, R. Gogoi, J. Wong, S. Mitragotri, J. Control. Release. 238 (2016) 176–185.
- [47] J.S. Suk, Q. Xu, N. Kim, J. Hanes, L.M. Ensign, Adv. Drug Deliv. Rev. 99 (2016) 28–51.

- [48] H. Cabral, Y. Matsumoto, K. Mizuno, Q. Chen, M. Murakami, et. al., Nat. Nanotechnol. 6 (2011) 815–823.
- [49] F. Schacher, E. Betthausen, A. Walther, H. Schmalz, D.V. Pergushov, A.H.E. Müller, ACS Nano. 3 (2009) 2095–2102.
- [50] Barenholz Y, J. Control. Release 160 (2012) 117–134.
- [51] B.A. Luxon, M. Grace, D. Brassard, R. Bordens, Int. J. Clin. Ther. Diagn. 24 (2002) 1363–1383.
- [52] R.D. Hamstra, JAMA. 243 (1980) 1726-1731.
- [53] E. Hinde, K. Thammasiraphop, H.T.T. Duong, J. Yeow, B. Karagoz, et. al., Nat. Nanotechnol. 12 (2017) 81–89.
- [54] J.A. Champion, S. Mitragotri, Proc. Natl. Acad. Sci. U.S.A. 103 (2006) 4930–4934.
- [55] D. Paul, S. Achouri, Y-Z. Yoon, J. Herre, C.E. Bryant, P. Cicuta. Biophys. J. 105, (2013) 1143-1150.
- [56] R. Agarwal, V. Singh, P. Jurney, L. Shi, S. V. Sreenivasan, K. Roy. Proc. Natl. Acad. Sci. U.S.A.110, (2013) 17247-17252.
- [57] J.D. Hartgerink, E. Beniash, S.I. Stupp, Proc. Natl. Acad. Sci. 99 (2002) 5133–5138.
- [58] Y. Geng, P. Dalhaimer, S. Cai, R. Tsai, M. Tewari, T. Minko, et. al., Nat. Nanotechnol. 2 (2007) 249–255.
- [59] J.M. DeSimone, J. Control. Release. 240 (2016) 541–543.
- [60] J. Xu, D.H.C. Wong, J.D. Byrne, K. Chen, C. Bowerman, J.M. DeSimone, Angew. Chem. Int. Ed Engl. 52 (2013) 6580–6589.
- [61] J.-H. Park, M.G. Allen, M.R. Prausnitz, J. Control. Release. 104 (2005) 51–66.
- [62] Y.-C. Kim, J.-H. Park, M.R. Prausnitz, Adv. Drug Deliv. Rev. 64 (2012) 1547–1568.
- [63] S. Wilhelm, A.J. Tavares, Q. Dai, S. Ohta, J. Audet, H.F. Dvorak, et. al., Nat. Rev. Mater. 1 (2016) 16014.
- [64] T. Sun, Y.S. Zhang, B. Pang, D.C. Hyun, M. Yang, Y. Xia, Angew. Chem. Int. Ed. Engl. (2014) 12520–12568.
- [65] W. Wang, S. Li, L. Mair, S. Ahmed, T.J. Huang, T.E. Mallouk, Angew. Chem. Int. Ed Engl. 53 (2014) 3265–3268.
- [66] M. Pal, N. Somalwar, A. Singh, R. Bhat, S.M. Eswarappa, D.K. Saini, et. al., Adv. Mater. 30 (2018) e1800429.
- [67] H. Xu, M. Medina-Sánchez, V. Magdanz, L. Schwarz, F. Hebenstreit, O.G. Schmidt, ACS Nano. 12 (2018) 327–337.
- [68] J. Li, B.E.-F. de Ávila, W. Gao, L. Zhang, J. Wang, Sci. Robotics. 2 (2017) eaam6431.
- [69] Z. Wu, L. Li, Y. Yang, P. Hu, Y. Li, S.-Y. Yang, et. al., Sci. Robotics. 4 (2019) eaax0613.
- [70] E. Gultepe, J.S. Randhawa, S. Kadam, S. Yamanaka, F.M. Selaru, E.J. Shin, et. al., Adv. Mater. 25 (2013) 514–519.
- [71] E. Gultepe, S. Yamanaka, K.E. Laflin, S. Kadam, Y. Shim, A.V. Olaru, et. al., Gastroenterol. 144 (2013) 691–693.
- [72] Y. Matsumura, H. Maeda, Cancer Res. 46 (1986) 6387–6392.
- [73] J. Fang, H. Nakamura, H. Maeda, Adv. Drug Deliv. Rev. 63 (2011) 136–151.
- [74] A.I. Minchinton, I.F. Tannock, Nat. Rev. Cancer. 6 (2006) 583–592.
- [75] R.K. Jain, T. Stylianopoulos, Nat. Rev. Clin. Oncol. 7 (2010) 653–664.
- [76] H. Chen, W. Zhang, G. Zhu, J. Xie, X. Chen, Nat. Rev. Mater. 2 (2017) 17024.
- [77] Q. Dai, S. Wilhelm, D. Ding, A.M. Syed, S. Sindhwani, Y. Zhang, et. al., ACS Nano. 12 (2018) 8423–8435.
- [78] T.P. Padera, A. Kadambi, E. di Tomaso, C.M. Carreira, E.B. Brown, Y. Boucher, et. al., Science, 296 (2002) 1883–1886.
- [79] M. Milosevic, A. Fyles, D. Hedley, R. Hill, Semin. Radiat. Oncol. 14 (2004) 249–258.
- [80] M. Hockel, K. Schlenger, B. Aral, M. Mitze, U. Schaffer, P. Vaupel, Cancer Res. 56 (1996) 4509–4515.
- [81] X.-D. Zhang, D. Wu, X. Shen, P.-X. Liu, N. Yang, B. Zhao, et. al., Int. J. Nanomed. 6 (2011) 2071–2081.
- [82] C. Hanley, A. Thurber, C. Hanna, A. Punnoose, J. Zhang, D.G. Wingett, Nanoscale Res. Lett. 4 (2009) 1409–1420.
- [83] W.-K. Oh, S. Kim, M. Choi, C. Kim, Y.S. Jeong, B.-R. Cho, et. al., ACS Nano. 4 (2010) 5301–5313.
- [84] B.D. Chithrani, A.A. Ghazani, W.C.W. Chan, Nano Lett. 6 (2006) 662-668.
- [85] X. Huang, L. Li, T. Liu, N. Hao, H. Liu, D. Chen, et. al., ACS Nano. 5 (2011) 5390–5399.
- [86] S. Hirn, M. Semmler-Behnke, C. Schleh, A. Wenk, J. Lipka, M. Schäffler, et. al., Eur. J. Pharm. Biopharm. 77 (2011) 407–416.
- [87] P.A. Netti, D.A. Berk, M.A. Swartz, A.J. Grodzinsky, R.K. Jain, Cancer Res. 60 (2000) 2497–2503.
- [88] T. Stylianopoulos, B. Diop-Frimpong, L.L. Munn, R.K. Jain, Biophys. J. 99 (2010) 3119–3128.
- [89] S. Ramanujan, A. Pluen, T.D. McKee, E.B. Brown, Y. Boucher, R.K. Jain, Biophys. J. 83 (2002) 1650–1660.
- [90] O. Trédan, C.M. Galmarini, K. Patel, I.F. Tannock, Natl. Cancer Inst. 99 (2007) 1441–1454.
- [91] A.J. Primeau, A. Rendon, D. Hedley, L. Lilge, I.F. Tannock, Clin. Cancer Res. 11 (2005) 8782–8788.

- [92] H. Lee, H. Fonge, B. Hoang, R.M. Reilly, C. Allen, Mol. Pharm. 7 (2010) 1195–1208.
- [93] K. Huang, H. Ma, J. Liu, S. Huo, A. Kumar, T. Wei, et. al., ACS Nano. 6 (2012) 4483-4493.
- [94] J. Wang, W. Mao, L.L. Lock, J. Tang, M. Sui, W. Sun, et. al., ACS Nano. 9 (2015) 7195–7206.
- [95] V.P. Chauhan, T. Stylianopoulos, J.D. Martin, Z. Popović, O. Chen, W.S. Kamoun, et. al., Nat. Nanotechnol. 7 (2012) 383–388.
- [96] A. Pluen, Y. Boucher, S. Ramanujan, T.D. McKee, T. Gohongi, E. di Tomaso, et. al., Proc. Natl. Acad. Sci. U.S.A. 98 (2001) 4628–4633.
- [97] T. Stylianopoulos, K. Soteriou, D. Fukumura, R.K. Jain, Ann. Biomed. Eng. 41 (2013) 68–77.
- [98] T. Stylianopoulos, M.-Z. Poh, N. Insin, M.G. Bawendi, D. Fukumura, L.L. Munn, et. al., Biophys. J. 99 (2010) 1342–1349.
- [99] O. Lieleg, R.M. Baumgärtel, A.R. Bausch, Biophys. J. 97 (2009) 1569–1577.
- [100] R.G. Thorne, A. Lakkaraju, E. Rodriguez-Boulan, C. Nicholson, Proc. Natl. Acad. Sci. U. S. A. 105 (2008) 8416–8421.
- [101] C.-H. Heldin, K. Rubin, K. Pietras, A. Östman, Nat. Rev. Cancer. 4 (2004) 806–813.
- [102] H.F. Dvorak, J.A. Nagy, D. Feng, L.F. Brown, A.M. Dvorak, Curr. Top. Microbiol. Immunol. (1999) 97–132.
- [103] L.T. Baxter, R.K. Jain, Microvasc. Res. 37 (1989) 77–104.
- [104] M. Wu, H.B. Frieboes, S.R. McDougall, M.A.J. Chaplain, V. Cristini, J. Lowengrub, J. Theor. Biol. 320 (2013) 131–151.
- [105] Y. Boucher, L.T. Baxter, R.K. Jain, Cancer Res. 50 (1990) 4478–4484.
- [106] R.K. Jain, Cancer Res. 47 (1987) 3039–3051.
- [107] K. Pietras, A. Ostman, M. Sjöquist, E. Buchdunger, R.K. Reed, C.H. Heldin, et. al., Cancer Res. 61 (2001) 2929–2934.
- [108] V.P. Chauhan, R.K. Jain, Nat. Mater. 12 (2013) 958–962.
- [109] A.A. Kalanuria, P. Nyquist, G. Ling, Vasc. Health Risk Manag. 8 (2012) 549–561.
- [110] S.C. Bergheanu, M.C. Bodde, J.W. Jukema, Neth. Heart J. 25 (2017) 231–242.
- [111] T.F. Whayne Jr, Int. J. Angiol. 20 (2011) 213–222.
- [112] R. Loeffen, H.M.H. Spronk, H. ten Cate, J. Thromb. Haemost. 10 (2012) 1207–1216.
- [113] A. Fabjan, F.F. Bajrović, Curr. Vasc. Pharmacol. 17 (2019) 29–34.
- [114] Y. Zheng, B. Belmont, A.J. Shih, Med. Eng. Phys. 38 (2016) 639–647.
- [115] M.E. DeBakey, Am. J. Cardiol. 63 (1989) 9-11.
- [116] N.I. Akkus, A. Abdulbaki, E. Jimenez, N. Tandon, Med. Devices. 8 (2015) 1–10.
- [117] T. Hinohara, M.R. Selmon, G.C. Robertson, L. Braden, J.S. Simpson, Circ. 81 (1990) IV79-91.
- [118] K. Kosuga, H. Tamai, K. Ueda, E. Kyo, S. Tanaka, T. Hata, et. al., Am. J. Cardiol. 87 (2001) 838–843.
- [119] E. Cavusoglu, A.S. Kini, J.D. Marmur, S.K. Sharma, Catheter. Cardiovasc. Interv. 62 (2004) 485–498.
- [120] J. Gorol, M. Tajstra, B. Hudzik, A. Lekston, M. Gasior, Postepy Kardiol. Adv. Interv. Cardiol. 14 (2018) 128– 134.
- [121] P. Bhatt, P. Parikh, A. Patel, M. Chag, A. Chandarana, R. Parikh, et. al., Cardiovasc. Revasc. Med. 16 (2015) 213–216.
- [122] Y. Sotomi, R.A. Shlofmitz, A. Colombo, P.W. Serruys, Y. Onuma, Interv. Cardiol. Rev. 11 (2016) 33.
- [123] J. Rawlins, J.N. Din, S. Talwar, O. Peter, Interv. Cardiol. Rev. 11 (2016) 27.
- [124] J. Toner, Y. Tu, Phys. Rev. Lett. 75 (1995) 4326-4329.
- [125] C.W. Reynolds, ACM SIGGRAPH Comput. Graph. 21 (1987) 25–34.
- [126] A. Hamel, C. Fisch, L. Combettes, P. Dupuis-Williams, C.N. Baroud, Proc. Natl. Acad. Sci. U.S.A. 108 (2011) 7290–7295.
- [127] P. Mandal, G. Patil, H. Kakoty, A. Ghosh, Acc. Chem. Res. 51 (2018) 2689–2698.
- [128] A.C. Hortelao, R. Carrascosa, N. Murillo-Cremaes, T. Patiño, S. Sanchez, ACS Nano 1 (2019) 429-439.
- [129] B. Esteban-Fernández de Ávila, D.E. Ramírez-Herrera, S. Campuzano, P. Angsantikul, L. Zhang, J. Wang, ACS Nano. 11 (2017) 5367–5374.
- [130] Y. Tu, F. Peng, A.A.M. André, Y. Men, M. Srinivas, D.A. Wilson, ACS Nano. 11 (2017) 1957–1963.
- [131] D. Kagan, S. Campuzano, S. Balasubramanian, F. Kuralay, G.-U. Flechsig, J. Wang, Nano Lett. 11 (2011) 2083–2087.
- [132] S. Balasubramanian, D. Kagan, C.-M.J. Hu, S. Campuzano, M.J. Lobo-Castañon, N. Lim, et. al., Angew. Chem. Int. Ed Engl. 50 (2011) 4161–4164.
- [133] M. Guix, J. Orozco, M. García, W. Gao, S. Sattayasamitsathit, A. Merkoçi, et. al., ACS Nano. 6 (2012) 4445–4451.
- [134] W. Gao, R. Dong, S. Thamphiwatana, J. Li, W. Gao, L. Zhang, J. Wang, ACS Nano. 9 (2015) 117–123.

- [135] Y. Tu, F. Peng, D.A. Wilson, Adv. Mater. 29 (2017) 1701970.
- [136] J. Wang, W. Gao, ACS Nano. 6 (2012) 5745–5751.
- [137] M. Guix, C.C. Mayorga-Martinez, A. Merkoçi, Chem. Rev. 114 (2014) 6285–6322.
- [138] P. Erkoc, I.C. Yasa, H. Ceylan, O. Yasa, Y. Alapan, M. Sitti, Adv. Ther. (2018) 1800064.
- [139] Y. Mei, G. Huang, A.A. Solovev, E.B. Ureña, I. Mönch, F. Ding, et. al., Adv. Mater. 20 (2008) 4085–4090.
- [140] W. Xi, A.A. Solovev, A.N. Ananth, D.H. Gracias, S. Sanchez, O.G. Schmidt, Nanoscale. 5 (2013) 1294–1297.
- [141] W. Gao, S. Sattayasamitsathit, J. Orozco, J. Wang, J. Am. Chem. Soc. 133 (2011) 11862–11864.
- [142] W.F. Paxton, S. Sundararajan, T.E. Mallouk, A. Sen, Angew. Chem. Int. Ed. 45(2006) 5420–5429.
- [143] X. Ma, K. Hahn, S. Sanchez, J. Am. Chem. Soc. 137 (2015) 4976–4979.
- [144] C. Chen, E. Karshalev, J. Guan, J. Wang, Small. 14 (2018) e1704252.
- [145] X. Wei, M. Beltrán-Gastélum, E. Karshalev, B. Esteban-Fernández de Ávila, J. Zhou, D. Ran, et al., Nano Lett. 19 (2019) 1914-1921.
- [146] W. Gao, A. Uygun, J. Wang, J. Am. Chem. Soc. 134 (2012) 897–900.
- [147] M. Zhou, T. Hou, J. Li, S. Yu, Z. Xu, M. Yin, et. al., ACS Nano. 13 (2019) 1324-1332.
- [148] T. Patiño, X. Arqué, R. Mestre, L. Palacios, S. Sánchez, Acc. Chem. Res. 51 (2018) 2662–2671.
- [149] X. Arqué, A. Romero-Rivera, F. Feixas, T. Patiño, S. Osuna, S. Sánchez, Nat. Commun. 10 (2019) 2826.
- [150] V. Magdanz, M. Medina-Sánchez, L. Schwarz, H. Xu, J. Elgeti, O.G. Schmidt, Adv. Mater. 29 (2017) 1606301.
- [151] R. Laocharoensuk, J. Burdick, J. Wang, ACS Nano. 2 (2008) 1069–1075.
- [152] W. Gao, S. Sattayasamitsathit, J. Wang, Chem. Rec. 12 (2012) 224–231.
- [153] S. Sanchez, A.N. Ananth, V.M. Fomin, M. Viehrig, O.G. Schmidt, J. Am. Chem. Soc.133, (2011) 14860-14863.
- [154] J. Li, S. Thamphiwatana, W. Liu, B.E-F. de Ávila, P. Angsantikul, E. Sandraz, et al., ACS Nano 10, (2016) 9536-9542.
- [155] E. Karshalev, Y. Zhang, B.E-F. de Ávila, M.B. Gastélum, Y. Chen, R. Mundaca-Uribe, et al., Nano Lett. (2019) 7816–7826.
- [156] S.K. Srivastava, M.M. Sánchez, B. Koch, O.G. Schmidt. Adv. Mater. 28, (2016) 832-837.
- [157] A. Ghosh, P. Fischer, Nano Lett. 9 (2009) 2243–2245.
- [158] L. Zhang, J.J. Abbott, L. Dong, B.E. Kratochvil, D. Bell, B.J. Nelson, Appl. Phys. Lett. 94 (2009) 064107.
- [159] A. Ghosh, D. Paria, H.J. Singh, P.L. Venugopalan, A. Ghosh, Phys. Rev. E Stat. Nonlin. Soft Matter Phys. 86 (2012) 031401.
- [160] A. Ghosh, D. Dasgupta, M. Pal, K.I. Morozov, A.M. Leshansky, A. Ghosh, Adv. Funct. Mater. 28 (2018) 1705687.
- [161] P.L. Venugopalan, R. Sai, Y. Chandorkar, B. Basu, S. Shivashankar, A. Ghosh, Nano Lett. 14 (2014) 1968–1975.
- [162] D. Schamel, A.G. Mark, J.G. Gibbs, C. Miksch, K.I. Morozov, A.M. Leshansky, et. al., ACS Nano. 8 (2014) 8794–8801.
- [163] D. Walker, B.T. Käsdorf, H.-H. Jeong, O. Lieleg, P. Fischer, Sci Adv. 1 (2015) e1500501.
- [164] Z. Wu, J. Troll, H.-H. Jeong, Q. Wei, M. Stang, F. Ziemssen, et. al., Sci. Adv. 4 (2018) eaat4388.
- [165] P. Mandal, A. Ghosh, Phys. Rev. Lett. 111 (2013) 248101.
- [166] P. Mandal, V. Chopra, A. Ghosh, ACS Nano. 9 (2015) 4717–4725.
- [167] A. Servant, F. Oiu, M. Mazza, K. Kostarelos, B.J. Nelson, Adv. Mater. 27 (2015) 2981–2988.
- [168] X. Yan, Q. Zhou, M. Vincent, Y. Deng, J. Yu, J. Xu, et. al., Sci. Robotics. 2 (2017) eaaq1155.
- [169] K.J. Rao, F. Li, L. Meng, H. Zheng, F. Cai, W. Wang, Small. 11 (2015) 2836–2846.
- [170] W. Wang, L.A. Castro, M. Hoyos, T.E. Mallouk, ACS Nano. 6 (2012) 6122–6132.
- [171] V. Garcia-Gradilla, J. Orozco, S. Sattayasamitsathit, F. Soto, F. Kuralay, A. Pourazary, et. al., ACS Nano. 7 (2013) 9232–9240.
- [172] S. Ahmed, W. Wang, L.O. Mair, R.D. Fraleigh, S. Li, L.A. Castro, et. al., Langmuir. 29 (2013) 16113–16118.
- [173] D. Kagan, M.J. Benchimol, J.C. Claussen, E. Chuluun-Erdene, S. Esener, J. Wang, Angew. Chem. Int. Ed Engl. 124 (2012) 7637–7640.
- [174] Y. Alapan, O. Yasa, O. Schauer, J. Giltinan, A.F. Tabak, V. Sourjik, et. al., Sci. Robotics. 3 (2018) eaar4423.
- [175] Y. Alapan, O. Yasa, B. Yigit, I. Ceren Yasa, P. Erkoc, M. Sitti, Annu. Rev. Control Robot. Auton. Syst. 2 (2018).
- [176] J. Han, J. Zhen, V. Du Nguyen, G. Go, Y. Choi, S.Y. Ko, et. al., Sci. Rep. 6 (2016) 28717.
- [177] Z. Wu, T. Li, J. Li, W. Gao, T. Xu, C. Christianson, et. al., ACS Nano. 8 (2014) 12041–12048.
- [178] O. Aydin, X. Zhang, S. Nuethong, G.J. Pagan-Diaz, R. Bashir, M. Gazzola, et al. Proc. Natl. Acad. Sci. U.S.A.

- 116, (2019) 19841-19847.
- [179] R. Mestre, T. Patiño, X. Barceló, S. Anand, A. Pérez-Jiménez, S. Sánchez. Adv. Mater. Technol. 4, (2019) 1800631.
- [180] M.M. Stanton, B.-W. Park, D. Vilela, K. Bente, D. Faivre, M. Sitti, et al. ACS Nano 11, (2017) 9968-9978.
- [181] M.M. Stanton, J. Simmchen, X. Ma, A. Miguel-López, S. Sánchez, Adv. Mater. Interfaces. 3 (2015) 1500505.
- [182] M.-R. Choi, K.J. Stanton-Maxey, J.K. Stanley, C.S. Levin, R. Bardhan, D. Akin, et. al., Nano Lett. 7 (2007) 3759–3765.
- [183] B.R. Smith, E.E.B. Ghosn, H. Rallapalli, J.A. Prescher, T. Larson, L.A. Herzenberg, et. al., Nat. Nanotechnol. 9 (2014) 481–487.
- [184] D. Akin, J. Sturgis, K. Ragheb, D. Sherman, K. Burkholder, J.P. Robinson, et. al., Nat. Nanotechnol. 2 (2007) 441–449.
- [185] O. Felfoul, M. Mohammadi, L. Gaboury, S. Martel, IEEE/RSJ Int. Conf. on Intell. Robots and Syst., IEEE (2011) 1304–1308.
- [186] O. Felfoul, M. Mohammadi, S. Taherkhani, D. de Lanauze, Y.Z. Xu, D. Loghin, et. al., Nat. Nanotechnol. 11 (2016) 941–947.
- [187] M. Kojima, Z. Zhang, M. Nakajima, T. Fukuda, Biomed. Microdevices. 14 (2012) 1027–1032.
- [188] V. Magdanz, S. Sanchez, O.G. Schmidt, Adv. Mater. 25 (2013) 6581–6588.
- [189] H. Yamaguchi, J. Wyckoff, J. Condeelis, Curr. Opin. in Cell Biol. 17 (2005) 559-564.
- [190] W. Wang, S. Goswami, E. Sahai, J.B. Wyckoff, J.E. Segall, J.S. Condeelis, Trends Cell Biol. 15 (2005) 138–145.
- [191] E. Sahai, Curr. Opin. Genet. Dev. 15 (2005) 87–96.
- [192] C. Bechinger, R. Di Leonardo, H. Löwen, C. Reichhardt, G. Volpe, G. Volpe, Rev. Mod. Phys. 88 (2016).
- [193] H.C. Berg, E. coli in Motion, Springer Sci. & Bus. Media, 2008.
- [194] J.-P. Bouchaud, A. Georges, Phys. Rep. 195 (1990) 127–293.
- [195] O. Chepizhko, F. Peruani, Phys. Rev. Lett. 111 (2013) 160604.
- [196] A.M. Leshansky, Phys. Rev. E Stat. Nonlin. Soft Matter Phys. 80 (2009) 051911.
- [197] J.K. Wróbel, S. Lynch, A. Barrett, L. Fauci, R. Cortez, J. Fluid Mech. 792 (2016) 775–797.
- [198] H.C. Berg, L. Turner, Nature 278 (1979) 349-351.
- [199] B.J. Nelson, K.E. Peyer, ACS Nano. 8 (2014) 8718–8724.
- [200] A. Ghosh, A. Ghosh, arXiv:1608.02253v1, 2016.
- [201] B. Liu, T.R. Powers, K.S. Breuer, Proc. Natl. Acad. Sci. U.S A. 108 (2011) 19516–19520.
- [202] Z. Xiao, M. Wei, W. Wang, ACS Appl. Mater. Interfaces. 11 (2019) 6667–6684.
- [203] J. Happel, H. Brenner, Low Reynolds number hydrodynamics, with special applications to particulate media, Vol. 1, (2012). Springer Sci. & Bus. Media, 2012.
- [204] E.M. Purcell, AIP Conf. Proc. (1976).
- [205] E. Lauga, T.R. Powers, Rep. on Prog. in Phys. 72 (2009) 096601.
- [206] J. Gray, G. J. Hancock, J. of Exp. Biol. 32 (1955) 802-814.
- [207] J. Elgeti, R.G. Winkler, G. Gompper, Rep. on Prog. in Phys. 78 (2015) 056601.
- [208] W. Wang, T.-Y. Chiang, D. Velegol, T.E. Mallouk, J. Am. Chem. Soc. 135 (2013) 10557–10565.
- [209] S.C. Takatori, W. Yan, J.F. Brady, Phys. Rev. Lett. 113 (2014) 028103.
- [210] T. Speck, R.L. Jack, Phys Rev E. 93 (2016) 062605.
- [211] S.C. Takatori, J.F. Brady, Curr. Opin. Colloid & Interface Sci. 21 (2016) 24–33.
- [212] F. Peng, Y. Men, Y. Tu, Y. Chen, D.A. Wilson, Adv. Funct. Mater. 28 (2018) 1706117.
- [213] I.S.M. Khalil, A.F. Tabak, K. Sadek, D. Mahdy, N. Hamdi, M. Sitti, IEEE Robot. Autom. Lett. 2 (2017) 927–934.
- [214] I.S.M. Khalil, D. Mahdy, A. El Sharkawy, R.R. Moustafa, A.F. Tabak, M.E. Mitwally, Klingner, et. al., IEEE Robot. Autom. Lett. 3 (2018) 1112–1119.
- [215] I.S.M. Khalil, A. Adel, D. Mahdy, M.M. Micheal, M. Mansour, N. Hamdi, et. al., APL Bioeng. 3 (2019) 026104.
- [216] D. Mahdy, R. Reda, N. Hamdi, I.S.M. Khalil, IEEE Instrum. & Meas. Mag. 21 (2018) 10–14.
- [217] G. Hwang, A.J. Paula, E.E. Hunter, Y. Liu, A. Babeer, B. Karabucak, et. al., Sci. Robot. 4 (2019) eaaw2388.
- [218] J. Wang, H.-J. Chen, T. Hang, Y. Yu, G. Liu, G. He, et. al., Nat. Nanotechnol. 13 (2018) 1078–1086.
- [219] J.H. Bahng, B. Yeom, Y. Wang, S.O. Tung, J. Damon Hoff, N. Kotov, Nature, 517 (2015) 596–599.
- [220] H. Zhou, J.-P. Kim, J.H. Bahng, N.A. Kotov, J. Lee, Adv. Funct. Mater. 24 (2014) 1439–1448.
- [221] T.G. Leong, C.L. Randall, B.R. Benson, N. Bassik, G.M. Stern, D.H. Gracias, Proc. Natl. Acad. Sci. U. S.A. 106 (2009) 703–708.

- [222] H.-J. Chen, C. Yang, T. Hang, G. Liu, J. Wu, D.-A. Lin, et. al., Sci. Rep. 8 (2018) 12600.
- [223] H.-J. Chen, T. Hang, C. Yang, G. Liu, D.-A. Lin, J. Wu, et. al., Nanoscale. 10 (2018) 1978–1986.
- [224] M. M. Sanchez, O Schmidt, Nature, 545(2017), 406-408.
- [225] X. Wang, X.-H. Qin, C. Hu, A. Terzopoulou, X.-Z. Chen, T.-Y. Huang, et. al., Adv. Funct. Mater. 28 (2018) 1804107.
- [226] K. Kobayashi, C. Yoon, S.H. Oh, J.V. Pagaduan, D.H. Gracias, ACS Appl. Mater. Interfaces. 11 (2019) 151–159.
- [227] J.M. Harris, J. Milton Harris, R.B. Chess, Nat. Rev. Drug Discov. 2 (2003) 214–221.
- [228] F.M. Veronese, G. Pasut, Drug Discov. Today. 10 (2005) 1451–1458.
- [229] S. Ding, C.P. O'Banion, J.G. Welfare, D.S. Lawrence, Cell Chem Biol. 25 (2018) 648–658.
- [230] J-J. Min, V. H. Nguyen, H-J Kim, Y. Hong, H.E. Choy. Nat. Protoc. 3 (2008) 629.
- [231] C.E. Badr, B.A. Tannous. Trends Biotechnol. 29 (2011) 624-633.
- [232] A. de la Zerda, J-W. Kim, E.I. Galanzha, S.S. Gambhir, V.P. Zharov. Contr. Med. & Mol. Imag Trends Cell Biol. 6 (2011) 346-369.
- [233] R. Weissleder. Science 312 (2006) 1168-1171.
- [234] M. Rudin, R. Weissleder. Nat. Rev. Drug Discov. 2 (2003) 123 131.
- [235] X. Ma, K. Hahn, S. Sanchez. J. Am. Chem. Soc. 137 (2015) 4976-4979.
- [236] X. Ma, S. Sanchez. Chem. Comm. 51 (2015) 5467-5470.
- [237] X. Ma, A. Jannasch, U-R. Albrecht, K. Hahn, A. Miguel-López, E. Schäffer, et al. Nano Lett. 15 (2015) 7043-7050.
- [238] M. Xuan, J. Shao, X. Lin, L. Dai, Q. He. ChemPhysChem 15 (2014) 2255-2260.
- [239] F. Soto, R. Chrostowski. Front. Bioengg. Biotechnol. 6 (2018).
- [240] S.K. Srivastava, G. Clergeaud, T.L. Andresen, A. Boisen. Adv. Drug Deliv. Rev. 138 (2019) 41-55.
- [241] Hosney A, Abdalla J, Amin IS, Hamdi N, Khalil ISM, Proc. IEEE RAS EMBS Int. Conf. Biomed. Robot. Biomechatron. (2016) 272–277.

Author Biographies



Arijit Ghosh is an Assistant Research Scientist in the Department of Chemical and Biomolecular Engineering at the Johns Hopkins University. He received his Ph.D in Electrical Communication Engineering from Indian Institute of Science, Bangalore in 2015 and his Bachelor of Engineering in Electronics and Telecommunication Engineering from Indian Institute of Engineering, Science and Technology in 2009. He has a decade long experience in the design and development of micro nanorobotic systems for biomedical engineering. Presently he is developing 3D reconfigurable microdevices for advanced clinical applications.



Weinan Xu is an assistant professor in the Department of Polymer Engineering at the University of Akron. He was a postdoctoral fellow in the Department of Chemical and Biomolecular Engineering at Johns Hopkins University. He received his PhD degree in Materials Science and Engineering from Georgia Institute of Technology in 2015, and his B.S. degree in Polymer Science and Engineering from Donghua University, China in 2011. His current research is focused on the development of hybrid materials, 3D structures and devices for their applications in biomedicine and energy conversion. He has been recognized with several awards including Excellence in Graduate Polymer Research Award from the American Chemical Society, Best PhD

Thesis Award from Sigma Xi and Georgia Tech, and Postdoctoral Fellow Research & Education Award from the Johns Hopkins University.



Neha Gupta is a junior in Chemical and Biomolecular Engineering major at Johns Hopkins University and active researcher in biomedical engineering and drug delivery.



David H. Gracias is a Professor at the Johns Hopkins University. He received his Ph.D. from the University of California at Berkeley in 1999 and did postdoctoral work at Harvard University, all in chemistry or related fields. His independent laboratory, since 2003, has pioneered the development of 3D and reconfigurable micro-, nano- and biodevices for miniaturized surgery and smart medicine. Prof. Gracias has co-authored over 175 technical publications, in addition to 32 issued patents.